Editor comments on ACP-2019-1169, 2nd revision of Kuilman et al.

The abstract and the manuscript reads now much better.

We thank the editor for her positive feedback and for her further comments.

On the abstract I have the following two comments (P1, L46):
(1) Abbreviation SST has not been introduced.
(2) Further, it has not been mentioned anywhere yet that changed SSTs have been considered. Either you add a sentence here or you add that the SSTs have been changed as well in line 32 where you write what is done is this study.

This has been implemented:

"In this study, we investigate the response of the middle atmosphere to a doubling of the CO_2-concentration and the associated changes in sea surface temperatures (SSTs) using the Whole Atmosphere Community Climate Model (WACCM)."

On the main text I have the following comments:
P5, L218: What do you mean with the latter is not considered in this study? No chemistry is considered!? Please rephrase the sentence to be clearer.
This sentence has been rephrased:

"The SSTs might be slightly different when they would be generated using a model that also includes atmospheric chemistry, however, this aspect is not considered in this study."

P5, L229-230: This sentence is also very weird. Why do they do not play a role in your experiments? The question from the referee was quite simple and could have been answered with yes or no. Either CFCs are considered or not. Since you use pre-industrial conditions I would assume that these are either zero or low since to my knowledge anthropogenic production (and thus the increase) of CFCs started later than 1850. This is something which can easily be checked. So please check and rephrase the sentence accordingly.
It has been checked the CFC are zero (there are some values 10^{-22} mol/mol, but mostly zeros), this also doesn't change between the control run and the perturbation runs. So, the short answer to the reviewer's question would be no, these are not considered.

The text has now been rewritten:

"The compset used in this experiment and all the following ones is still F_1850, which means that other radiatively and chemically active gases, such as ozone, will change only because of the changes in the CO_2-concentration, due to WACCM's interactive chemistry. This also means that the effects of chlorofluorocarbons (CFCs) are not considered in our experiments, as anthropogenic production of CFCs started later than 1850."

P6, Table 1: The naming in the table is quite misleading and I needed a while to understand how your four experiments differentiate from each other. I would suggest to do the following change (and simplification) to the table to be clearer:
Experiment CO2 SSTs
C1 PI PI
C2 double PI
S1 PI double (or high)
S2 double double (or high)
The simplification has been implemented.

Further, it would be more logical if the naming would be C1, S1, S2 and S3 since you have one control run and three scenarios.
This has been implemented.

P7, L298-312: This text part is also quite difficult to read. I would suggest that you repeat here the sentences from the appendix what R, S and the deltas are.
This has been implemented.
"In which $\vec{R}$ represents the vertical profile of the net long-wave radiation emitted by each layer in the atmosphere and by the surface. $\vec{S}$ is the vertical profile of the solar radiation absorbed by each layer. The matrix $\left(\frac{\partial \vec{R}}{\partial \vec{T}}\right)$ is the Planck feedback matrix, in which the vertical profiles of the changes in the divergence of radiative energy fluxes due to a temperature change are represented. ΔT represents the temperature change."

Further, I would suggest to move the second paragraph to the appendix or to make a list with bullets for CO2, H2O, O3, cloud and Albedo where then is written what has been done for each species or you just simplify the text. In general the difference between control and experiment is considered, so just mention then what is the difference for the species. In your text especially the phrase "the other variables" is not clear and rather confusing.
The authors agree that the former formulation was confusing. The following has been added to the appendix:

The factors $\Delta(\vec{S} - \vec{R})_{CO_2}$, $\Delta(\vec{S} - \vec{R})_{O_3}$, $\Delta(\vec{S} - \vec{R})_{H_2O}$, $\Delta(\vec{S} - \vec{R})_{albedo}$ and $\Delta(\vec{S} - \vec{R})_{cloud}$ in eqs (1-5) are calculated by inserting the output variables from WACCM in the radiation code of CFRAM. Here, one takes the output variables from the control run, apart from the variable that is related to the direct forcing or the feedback. The table below shows which variables have been taken from the perturbation runs for each feedback.

Direct forcing/feedback	Changed variables in the radiation code
CO$_2$	CO$_2$
Ozone	O$_3$
Water vapour	Specific humidity Surface pressure Surface temperature Dew point temperature
Albedo	Downwelling solar flux at surface

	Net solar flux at surface
Cloud	Cloud fraction
	Cloud ice
	Cloud liquid amount

Table A1: The variables from the perturbation runs inserted in the radiation code of CFRAM to calculate the temperature change in response to the changes in CO_2, O_3, water vapour, cloud and albedo.

The main text now refers to the appendix in the following way:

Here, one takes the output variables from the control run, apart from the variable that is related to the direct forcing or the feedback. Table A1 in the Appendix shows which variables from the perturbation runs have been inserted in the radiation code of CFRAM in order to calculate $\Delta(\vec{S} - \vec{R})_{CO_2}$, $\Delta(\vec{S} - \vec{R})_{O_3}$, $\Delta(\vec{S} - \vec{R})_{H_2O}$, $\Delta(\vec{S} - \vec{R})_{albedo}$ and $\Delta(\vec{S} - \vec{R})_{cloud}$ and eventually the associated temperature changes.

P9, 392: add "(C1)" after control simulation.
This has been added (also for the other simulations):

"Figure 1: The total change in temperature in July (top) and January (bottom) for (a,d) the simulation with high CO_2 and SSTs (S3), (b,e) the simulation with high CO_2 (S1), (c,f) the simulation with high SSTs (S2), all as compared to the pre-industrial control simulation (C1). The dotted regions indicate the regions where the data reaches a confidence level of 95%. The black line indicates the tropopause height for the experiments S3 (a,d), S1 (b,e) and S2 (c,f)."

P14, Figure 5 caption: Shouldn't it read "S1 - C1" and "C2 - C1", respectively? The same holds for Fig7, Fig 9, Fig. 10, Fig 11 and Fig 13.
Thanks for this comment, this was indeed incorrect. It has now been corrected.

P18, L697: Be more precise than "higher up". Above which level?
This has been clarified:

"Fig. 8 shows that above 1 hPa, there are also large percentage changes in water vapour. However, the absolute concentration of water vapour is small there, which explains why there is no temperature response to these changes."

P24, L870: Sentence not clear. Please rephrase. Which exact mechanism are you talking about? What exactly is out of the scope of the paper? Do you mean to investigate the exact mechanism why the non-LTE effects are small is outside the scope of the paper?
This has been rewritten:
"We find that there are also some small temperature changes due to non-LTE effect above 0.1 hPa. How the non-LTE effects exactly cause the small temperature changes in this region is outside the scope of this paper and needs further investigation."

P26, L897: Which errors? Do you mean the bars in the bar chart of Figure 13?

Yes, that is correct. I have made this clearer in the text.

"As in Fig. 11, the 'Error'-column in Fig. 13 shows the difference between temperature change in WACCM and the sum of the calculated temperature responses in CFRAM."

We have also clarified this bit in the description in Fig. 11:

"This term shows the difference between temperature change in WACCM and the sum of the calculated temperature responses in CFRAM (see eq. 9 in section 2.3)."

P30, L1122: What is the PRP method? Please add more details.

This method and abbreviation had introduced in the introduction. Now more details have been given at this point in the paper as well:

"This is also commonly done in the partial radiative perturbation (PRP) method, in which partial derivatives of the model top of the atmosphere radiation are evaluated with respect to changes in model parameters by diagnostic rerunning the model's radiation code (Bony et al., 2006)."

Other technical issues:

P2, L64: the -> this
This has been corrected.

P3, L122: these -> "the" or "the respective"
This has been corrected.

P3, L126: use plural, thus "forcing and feedbacks"
This has been corrected.

P3, L143: such idealized -> such "an" idealized
This has been corrected.

P6, L264: effect -> affect
This has been corrected.

P9, L391: add "to" before "the"
This has been corrected.

P10, L433: Past should be used here: "In this section, we have discussed......."
It was meant to be in the current section (4), we will discuss. This has now been changed in the text to make it clearer:

"In the following subsections 4.1-4.5, we will discuss the meridional-vertical profiles of the temperature responses to the direct forcing and the various feedbacks during

P10, L444: add "is found" after CO2-concentration.
This has been added.

P11, L452: singular should be used here -> run
This has been corrected.

P13, L536: add "by" so that it reads "could be caused by an increase…."
This has been corrected.

P14, L545: add "the" so that it reads "….due to the……".
This has been corrected.

P15, L589: add "scale" so that it reads "……..synoptic scale waves"
This has been added.

P16, L645: add "concentration" after CO2.
This has been added.

P17, L652: add "to" before "the" so that it reads "…with respect to the….."
This has been added.

P18, L698: add "vapour" so that it reads "water vapour".
This has been added.

P20, L759: stratosphere -> stratospheric
This has been corrected.

P20, L760: until -> up to
This has been changed.

P21, L771: add "average" so that it reads "by taking the average in this way".
This has been changed:

"By calculating the average in this way, we can directly compare the vertical values in different regions of the atmosphere."

P22, L814: add "is" so that it reads "is a bit smaller".
This has been added.

P22, L822-824: "before" appears in the sentence twice. I would suggest to delete the latter one.
The latter 'before' has been removed.

P22, L832: move "mostly" before "contributes" so that it reads "which mostly contributes…".
'Mostly' has been moved.

P24, L874: "for due" is not correct, this "for" is obsolete here. Please remove.
'For' has been removed.

P26, L890: add "the" so that it reads "shows the"
'The' has been added.

P26, L931-932: "before" twice. One is therefore obsolete. I would suggest to remove the latter one.
'Before' has been removed.

Using the climate feedback response method to quantify climate feedbacks in the middle atmosphere in WACCM

Maartje Sanne Kuilman[1], Qiong Zhang[2], Ming Cai[3], Qin Wen[1,4]

1. Department of Meteorology and Bolin Centre for Climate Research, Stockholm University, Stockholm, Sweden
2. Department of Physical Geography and Bolin Centre for Climate Research, Stockholm University, Stockholm, Sweden
3. Department of Earth, Ocean and Atmospheric Science, Florida State University, Tallahassee, Florida, USA
4. Laboratory for Climate and Ocean-Atmosphere Studies (LaCOAS), Department of Atmospheric and Oceanic Sciences, School of Physics, Peking University, Beijing, China

Corresponding author: Maartje Sanne Kuilman (maartje.kuilman@misu.su.se)

Abstract

Over recent decades it has become clear that the middle atmosphere has a significant impact on surface and tropospheric climate. A better understanding of the middle atmosphere and how it reacts to the current increase of the concentration of carbon dioxide (CO_2) is therefore necessary. In this study, we investigate the response of the middle atmosphere to a doubling of the CO_2-concentration and the associated changes in sea surface temperatures (SSTs) using the Whole Atmosphere Community Climate Model (WACCM). We use the climate feedback response analysis method (CFRAM) to calculate the partial temperature changes due to an external forcing and climate feedbacks in the atmosphere. As this method has the unique feature of additivity, these partial temperature changes are linearly addable. In this study, we discuss the direct forcing of CO_2 and the effects of the ozone, water vapour, cloud, albedo and dynamical feedbacks.

As expected, our results show that the direct forcing of CO_2 cools the middle atmosphere. This cooling becomes stronger with increasing height: the cooling in the upper stratosphere is about three times as strong as the cooling in the lower stratosphere. The ozone feedback yields a radiative feedback that mitigates this cooling in most regions of the middle atmosphere. However, in the tropical lower stratosphere and in some regions of the mesosphere, the ozone feedback has a cooling effect. The increase in CO_2-concentration causes the dynamics to change. The temperature response due to this dynamical feedback is small in the global average, although there are large temperature changes due to this feedback locally. The temperature change in the lower stratosphere is influenced by the water vapour feedback and to a lesser degree by the cloud and albedo feedback. These feedbacks play no role in the upper stratosphere and the mesosphere. We find that the effects of the changed SSTs on the middle atmosphere are relatively small as compared to the effects of changing the CO_2. However, the changes in SSTs

Deleted: to a doubling CO_2 in

50   are responsible for dynamical feedbacks that cause large temperature
51   changes. Moreover, the temperature response to the water vapour feedback
52   in the lower stratosphere is almost solely due to changes in the SSTs. As
53   CFRAM has not been applied to the middle atmosphere in this way before,
54   this study also serves to investigate the applicability as well as the limitations
55   of this method. This work shows that CFRAM is a very powerful tool to study
56   climate feedbacks in the middle atmosphere. However, it should be noted that
57   there is a relatively large error term associated with the current method in the
58   middle atmosphere, which can be for a large part be explained by the
59   linearization in the method.
60
61   **1. Introduction**
62
63   The increase of concentration of carbon dioxide in the atmosphere forms a
64   major perturbation to the climate system. It is commonly associated with
65   lower-atmospheric warming. However, in the middle atmosphere, the increase
66   of CO_2 leads to a cooling of this region instead. This cooling has been well
67   documented and is found by both model studies and observations (e.g.
68   *Manabe and Wetherald*, 1975; *Ramaswamy et al.*, 2001; *Beig et al.,* 2003).
69
70   The middle atmosphere is not only affected by the increase in CO_2-
71   concentration, but also by the decrease in ozone-concentration. The depletion
72   of ozone (O_3) also effects the temperature in the stratosphere and leads to a
73   cooling (*Shine et al,* 2003). A better understanding of the effect of the
74   increased CO_2-concentration on the middle atmosphere, will help to
75   distinguish the effects of the changes CO_2- and O_3-concentration.
76
77   Another major motivation for this study is the emerging evidence that the
78   middle atmosphere has an important influence on surface and tropospheric
79   climate (*Shaw and Shepherd*, 2008). It has, for example, been shown that
80   cold winters in Siberia are linked to changes in the stratospheric circulation
81   (*Zhang et al.*, 2018).
82
83   *Nowack et al.* (2015) has found that there is an increase in global mean
84   surface warming of about 1°C when the ozone is prescribed at pre-industrial
85   levels, as compared with when it is evolving in response to an abrupt 4xCO_2
86   forcing. It should be noted that the exact importance of changes in ozone
87   seems to be dependent on both the model and the scenario (*Nowack et al*.,
88   2015) and is not found by all studies (*Marsh et al.*, 2016).
89
90   As the effect is found to be rather large in some studies, and absent in other,
91   there is a need for a better understanding of the behaviour of the middle
92   atmosphere in response to changing CO_2 conditions, as the ozone
93   concentration is influenced by this. Ozone is an example of a climate
94   feedback, a process that changes in response to a change in CO_2-
95   concentration and in turn dampens or amplifies the climate response to the
96   CO_2 perturbation.
97
98   These climate feedbacks are a challenging subject of study, as observed
99   climate variations might not be in equilibrium, multiple processes are

Deleted: the

2

101 operating at the same time and moreover the geographical structures and
102 timescales of different forcings differ. However, feedbacks form a crucial part
103 of understanding the response of the atmosphere to changes in the CO_2-
104 concentration.

105 Various methods have been developed to study these feedbacks, such as the
106 partial radiative perturbation (PRP) method, the online feedback suppression
107 approach and the radiative kernel method (*Bony et al.,* 2006 and the
108 references therein). These methods study the origin of the global climate
109 sensitivity (*Soden and Held*, 2006; *Caldwell et al.*, 2016; *Rieger et al.*, 2017).
110 The focus of these methods is on changes in the global mean surface
111 temperature, global mean surface heat and global mean sensible heat fluxes
112 (*Ramaswamy et al., 2019*).

113 These methods are powerful for this purpose; however, they are not suitable
114 to explain temperature changes on spatially limited domains. They neglect
115 non-radiative interactions between feedback processes and they only account
116 for feedbacks that directly affect the radiation at the top of the atmosphere
117 (TOA).

118 The climate feedback-response analysis method (CFRAM) is an alternative
119 method which takes into account that the climate change is not only
120 determined by the energy balance at the top of the atmosphere, but is also
121 influenced by the energy flow within the Earth's system itself (*Cai and Lu,*
122 *2009, Lu and Cai*, 2009). The method is based on the energy balance in an
123 atmosphere-surface column. It solves the linearized infrared radiation transfer
124 model for the individual energy flux perturbations. This makes it possible to
125 calculate the partial temperature changes due to an external forcing and the
126 internal feedbacks in the atmosphere. It has the unique feature of additivity,
127 such that these partial temperature changes are linearly addable.
128
129 As a practical diagnostic tool to analyse the role of various forcings and
130 feedbacks, CFRAM has been used widely in climate change research on
131 studying surface climate change (*Taylor et al.,* 2013; *Song and Zhang,* 2014;
132 *Hu et al.,* 2017; *Zheng et al.,* 2019). CFRAM has been applied to study the
133 middle atmosphere climate sensitivity as well (*Zhu et al.,* 2016). In their study,
134 Zhu et al. *(2016)* have adapted CFRAM and applied it to both model output,
135 as well as observations. The atmospheric responses during solar maximum
136 and minimum were studied and it was found that the variation in solar flux
137 forms the largest radiative component of the middle atmosphere temperature
138 response.
139
140 In the present work, we apply CFRAM to climate sensitivity experiments
141 performed with the Whole Atmosphere Community Climate Model (WACCM),
142 which is a high-top global climate system model, including the full middle
143 atmosphere chemistry.
144
145 We investigate the middle atmosphere response to CO_2-doubling. We
146 acknowledge that such an idealized equilibrium simulation cannot reproduce
147 the complexity of the atmosphere, in which the CO_2-concentration is changing

Deleted: these

Deleted: forcing

Deleted: feedback

151 gradually. However, simulating a double CO_2-scenario still allows us to
152 identify robust feedback processes in the middle atmosphere.
153
154 There are two aspects of the middle atmosphere response to CO_2-doubling:
155 there is the effect of the changes in CO_2-concentration directly, as well as the
156 changes in sea surface temperature (SST) which are in itself caused by the
157 changes in CO_2-concentration. It is useful to investigate these aspects
158 separately, as former should be robust, while the effect of the changed SST
159 depends on the changes in tropospheric climate, which can be expected to
160 depend more on the model.
161
162 In this study, we investigate the effects of doubling the CO_2-concentration and
163 the accompanying sea surface temperature change on the temperature in the
164 middle atmosphere as compared to the pre-industrial state. We use CFRAM
165 to calculate the radiative contribution to the temperature change due to
166 changes in carbon dioxide directly as well as due to changes in ozone, water
167 vapour, albedo and clouds. We refer to the changes in ozone, water vapour,
168 albedo and clouds in response to changes in the CO_2-concentration as the
169 ozone, water vapour, albedo and cloud feedbacks.
170
171 The circulation in the middle atmosphere is driven by waves. Wave forcing
172 drives the temperatures in the middle atmosphere far away from radiative
173 equilibrium. In the mesosphere, there is a zonal forcing, which yields a
174 summer to winter transport. In the polar winter stratosphere, there is a strong
175 forcing that consists of rising motion in the tropics, poleward flow in the
176 stratosphere and sinking motion in the middle and high latitudes. This
177 circulation is referred to as the 'Brewer-Dobson circulation' (*Brewer,* 1949;
178 *Dobson*, 1956).
179
180 Dynamical effects make important contributions to the middle-atmosphere
181 energy budget, both through eddy heat flux divergence and through adiabatic
182 heating due to vertical motions. It is therefore important that we also consider
183 changes to the middle-atmosphere climate due to dynamics. We refer to this
184 as the 'dynamical feedback' (*Zhu et al*., 2016).

184 The main goal of this paper is to calculate the contribution to the temperature
185 change due to changes in carbon dioxide directly as well as due to changes in
186 ozone, water vapour, albedo, clouds and dynamics in the middle atmosphere
187 under a double CO_2-scenario using CFRAM. Our intention is not to give a
188 complete account of the exact mechanisms behind the changes in ozone,
189 water vapour, albedo, clouds and dynamics.

190 **2. The model and methods**
191
192 **2.1 Model description**

193 The Whole Atmosphere Community Model (WACCM) is a chemistry-climate
194 model, which spans the range of altitudes from the Earth's surface to about
195 140 km (*Marsh et al.,* 2013). The model consists of 66 vertical levels with
196 irregular vertical resolution, which ranges from ~1.1 km in the troposphere,

Deleted: ,

198 1.1–1.4 km in the lower stratosphere, 1.75 km at the stratosphere and 3.5 km
199 above 65 km. The horizontal resolution is 1.9° latitude by 2.5° longitude.

200 WACCM is a superset of the Community Atmospheric Model version 4
201 (CAM4) developed at the National Center for Atmospheric Research (NCAR).
202 Therefore, WACCM includes all the physical parameterizations of CAM4
203 (*Neale et al.,* 2013), and a well-resolved high-top middle atmosphere. The
204 orographic gravity wave (GW) parameterization is based on *McFarlane*
205 (1987). WACCM also includes parameterized non-orographic GWs, which are
206 generated by frontal systems and convection (*Richter et al.,* 2010). The
207 parameterization of non-orographic GW propagation is based on the
208 formulation by *Lindzen* (1981).

209 The chemistry in WACCM is based on version 3 of the Model for Ozone and
210 Related Chemical Tracers (MOZART3). This model represents chemical and
211 physical processes from the troposphere until the lower thermosphere.
212 (*Kinnison et al.,* 2007). In addition, WACCM simulates chemical heating,
213 molecular diffusion and ionization and gravity wave drag.

214 **2.2 Experimental set-up**

215 In this study, the F_1850 compset (component set) of the model is used, i.e.
216 the model assumes pre-industrial (PI) conditions. This compset simulates an
217 equilibrium state, which means that it runs a perpetual year 1850. Four
218 experiments have been performed for this study (see Table 1).

219 Experiment C1 is the control run, with the pre-industrial CO_2 concentration
220 (280 ppm) and forced with pre-industrial ocean surface conditions such as
221 sea surface temperatures and sea ice. These SSTs are generated from the
222 CMIP5 pre-industrial control simulation by the fully coupled Earth system
223 model CESM. The atmospheric component of CESM is the same as WACCM,
224 but does not include stratospheric chemistry (*Hurrell et al.,* 2013). The SSTs
225 might be slightly different when they would be generated using a model that
226 also includes atmospheric chemistry, however, this aspect is not considered
227 in this study.

228 Experiment S1 represents the experiment with the CO_2 concentration doubled
229 as compared to the pre-industrial state (560 ppm) and forced with the same
230 pre-industrial SSTs as in experiment C1. In WACCM, the CO_2-concentration
231 does not double everywhere in the atmosphere. Only the surface level CO_2
232 mixing ratio is doubled, and elsewhere in the atmosphere is calculated
233 according to WACCM's chemical model.

234 The compset used in this experiment and all the following ones is still F_1850,
235 which means that other radiatively and chemically active gases, such as
236 ozone, will change only because of the changes in the CO_2-concentration,
237 due to WACCM's interactive chemistry. This also means that the effects of
238 chlorofluorocarbons (CFCs) are not considered in our experiments, as
239 anthropogenic production of CFCs started later than 1850.

Deleted: temperature

Deleted: (referred to SSTs from now on).

Deleted: This latter

Deleted: C2

Deleted: Chlorofluorocarbons

Deleted:), which have a major impact on the ozone concentration in the real atmosphere, don't play a role

In experiment S2, we simulate the scenario, in which there is the SSTs forcing from the coupled CESM for double CO_2 condition. This means that the sea surface temperatures are higher than in the PI run, and there is less sea ice. However, in this experiment the CO_2-concentration is kept at the pre-industrial value of 280 ppm. S3 represents the experiment with the CO_2-concentration in the atmosphere doubled to 560 ppm and the SSTs prescribed for the double CO_2-climate. Experiment C1, S1, S2 and S3 will be also referred to hereafter by PI, the simulation with high CO2, the simulation with high SSTs and the simulation with high CO_2 and SSTs, respectively.

The experimental setup of this study is similar to the setup performed with the Canadian Middle Atmosphere Model (CMAM) *by Fomichev et al.* (*2007*) and with the Hamburg Model of the Neutral and Ionized Atmosphere (HAMMONIA) by *Schmidt et al.* (2006). The HAMMONIA model is coupled to the same chemical model as WACCM: MOZART3. The setup in their study is similar, however, in their study, they double the CO_2-concentration from 360 ppm to 720 ppm, while in our study, we double from the pre-industrial level of CO_2 (280 ppm).

Note that experiment S2 and S1 are not representing scenarios that could happen in the real atmosphere. These experiments have been used to study the effect of the SSTs separately. Experiment S3 doesn't take into account other (anthropogenic) changes in the atmosphere not caused by changes in the CO_2-concentration and the SSTs.

All the simulations are run for 50 years, of which the last 40 years are used for analysis. In the all results shown, we have used the 40 year mean of our model data.

Table 1. Set-up of the model experiments.

Experiment	CO_2	SSTs from CESM equilibrium run
C1	PI	PI
S1	Double	PI
S2	PI	High
S3	Double	High

2.3 Climate feedback-response analysis method (CFRAM)

In this study, we aim to quantify the different climate feedbacks that may play a role in the middle atmosphere in a double CO_2-climate. For this purpose, we apply the climate feedback-response analysis method (CFRAM) (*Lu and Cai*, 2009).

As briefly discussed in the introduction, traditional methods to study climate feedbacks are based on the energy balance at the top of the atmosphere (TOA). This means that the only climate feedbacks that are taken into consideration are those that affect the radiative balance at the TOA. However, there are other thermodynamic and dynamical processes that do not directly affect the TOA energy balance, while they do yield a temperature response in

6

308   the atmosphere.
309
310   Contrary to TOA-based methods, CFRAM considers all the radiative and non-
311   radiative feedbacks that result from the climate system due to response to an
312   external forcing. This means that CFRAM starts from a slightly different
313   definition of a feedback process. Note also that as the changes in temperature
314   are calculated simultaneously, the vertical mean temperature or lapse rate
315   feedback per definition do not exist in CFRAM.
316
317   Another advantage of CFRAM is that it allows for measuring the magnitude of
318   a certain feedback in units of temperature. We can actually calculate how
319   much of the temperature change is due to which process. The *'climate*
320   *response'* in the name of this method refers to the changes in temperature in
321   response to the climate forcings and climate feedbacks.
322
323   We refer to the Appendix for the complete formulation of CFRAM diagnostics
324   using outputs of WACCM. Based on the linear decomposition principle, we
325   can solve Eq. (A12) for each of the terms on its right-hand side. This yields
326   the partial temperature changes due to each specific process namely:
327

328    $$\Delta T_{CO_2} = \left(\frac{\partial R}{\partial T}\right)^{-1} \Delta\left(S - R\right)_{CO_2} \tag{1}$$

329

330    $$\Delta T_{O_3} = \left(\frac{\partial R}{\partial T}\right)^{-1} \Delta\left(S - R\right)_{O_3} \tag{2}$$

331

332    $$\Delta T_{H_2O} = \left(\frac{\partial R}{\partial T}\right)^{-1} \Delta\left(S - R\right)_{H_2O} \tag{3}$$

333

334    $$\Delta T_{albedo} = \left(\frac{\partial R}{\partial T}\right)^{-1} \Delta\left(S - R\right)_{albedo} \tag{4}$$

335

336    $$\Delta T_{cloud} = \left(\frac{\partial R}{\partial T}\right)^{-1} \Delta\left(S - R\right)_{cloud} \tag{5}$$

337
338   In which R represents the vertical profile of the net long-wave radiation
339   emitted by each layer in the atmosphere and by the surface. S is the vertical
340   profile of the solar radiation absorbed by each layer. The matrix $\left(\frac{\partial R}{\partial T}\right)$
341   is the Planck feedback matrix, in which the vertical profiles of the changes in
342   the divergence of radiative energy fluxes due to a temperature change are
343   represented. ΔT represents the temperature change.
344
345   The factors $\Delta\left(S - R\right)_{CO_2}$, $\Delta\left(S - R\right)_{O_3}$, $\Delta\left(S - R\right)_{H_2O}$, $\Delta\left(S - R\right)_{albedo}$ and
346    $\Delta\left(S - R\right)_{cloud}$ are calculated by inserting the output variables from WACCM in
347   the radiation code of CFRAM. Here, one takes the output variables from the
348   control run, apart from the variable that is related to the direct forcing or the
349   feedback. Table A1 in the Appendix shows which variables from the
350   perturbation runs have been inserted in the radiation code of CFRAM in order

Formatted: Font colour: Text 1

to calculate $\Delta(S-R)_{CO_2}$, $\Delta(S-R)_{O_3}$, $\Delta(S-R)_{H_2O}$, $\Delta(S-R)_{albedo}$ and $\Delta(S-R)_{cloud}$ and eventually the associated temperature changes.

Similarly, to equations (1)-(5), we also calculate the temperature change due to non-local thermal equilibrium (non-LTE) processes and the dynamical feedback. We calculate the terms $\Delta(S-R)_{non-LTE}$ and Δdyn in Eq. (A4) and (A7).

$$\Delta T_{non-LTE} = \left(\frac{\partial R}{\partial T}\right)^{-1}\Delta(S-R)_{non-LTE} \qquad (6)$$

$$\Delta T_{dyn} = \left(\frac{\partial R}{\partial T}\right)^{-1}\Delta dyn \qquad (7)$$

The calculated partial temperature changes can be added, their sum being equal to the total temperature change. It is important to note that this does not mean that the individual processes are physically independent of each other.

$$\Delta T_{CFRAM} = + \Delta T_{O_3} + \Delta T_{H_2O} + \Delta T_{albedo} + \Delta T_{cloud} + \Delta T_{non-LTE} + \Delta T_{dyn} \qquad (8)$$

The linearization done for equations (A9) and (A10) introduces an error between the temperature difference as calculated by CFRAM and as seen in the model output. Another source of error is that the radiation code of the CFRAM calculations is not exactly equal to the radiation code of WACCM.

$$\Delta T_{CFRAM} = \Delta T_{WACCM} - \Delta T_{error} \qquad (9)$$

For more details on the CFRAM method, please refer to *Lu and Cai* (2009).

Note that the method used in this study differs from the Middle Atmosphere Climate Feedback Response Analysis Method (MCFRAM) used by *Zhu et al.* (2016). The major difference is that in this study, we perform the calculations using the units of energy fluxes (Wm^{-2}) instead of converting to heating rates (Ks^{-1}). In other words, we use Wm^{-2} as the units of heating rates for the layer between two adjacent vertical levels. Because the radiative heating rates are the net radiative energy fluxes entering the layer, it is rather natural and straightforward (i.e., without dividing the mass in the layer to convert it to units of Ks^{-1}) to have the same units of heating rates (convergence) as the radiative energy fluxes. Another difference is that our method is not applicable above 0.01 hPa (~80 km), while *Zhu et al.* (2016) added molecular thermal conduction to the energy equation, to perform the calculations beyond the mesopause.

3. Temperature responses in a double CO$_2$ scenario

As described in section 2.2, four experiments were performed with WACCM: a simulation with pre-industrial conditions (experiment C1) , a simulation with changed SSTs only (experiment S2), a simulation with only a changed CO$_2$-

415 concentration (experiment S1) and a final simulation with both changed SSTs
416 and CO_2-concentration (experiment S3).

417

418 Figure 1 shows the zonal mean temperature changes for the different
419 experiments with respect to the pre-industrial state, as modelled by WACCM.
420 The results reach a statistical significance of 95% for the whole middle
421 atmosphere domain in the experiments S3-C1 and S1-C1, and most of the
422 middle atmosphere for experiment S2-C1. For this figure, as well as for all the
423 results shown in this paper, we have used the 40 year mean of our data.

424

425 In line with what was shown in earlier studies (e.g. *Akmaev*, 2006; *Fomichev*
426 *et al.*, 2007), we observe that an increase in CO_2 causes a cooling in the
427 middle atmosphere with the exception of the cold summer upper mesosphere
428 region. We also observe that changing the SSTs alone, while leaving the
429 CO_2-concentration at the pre-industrial levels (Fig 1c and 1f) also yields
430 significant temperature changes over a large part of the middle atmosphere
431 and contributes to the observed warming in the cold summer mesopause
432 region.

433

434 As found previously by *Fomichev et al.* (2007) and *Schmidt et al.* (2006), we
435 find that the sum of the two separate temperature changes in the experiment
436 with changed CO_2 only and changed SSTs only (experiment S1 and S2) is
437 approximately equal to the changes observed in the combined simulation
438 (experiment S3). *Shepherd* (2008) has explained this phenomenon as follows:
439 climate change affects the middle atmosphere in two ways: either radiatively
440 through in situ changes associated with changes in CO_2 or dynamically
441 through changes in stratospheric wave forcing, which are primarily a result of
442 changing the SSTs (*Shepherd,* 2008). Even though the radiative and dynamic
443 processes are not independent, these processes are seen to be
444 approximately additive (*Sigmond et al.*, 2004, *Schmidt et al.,* 2006, *Fomichev*
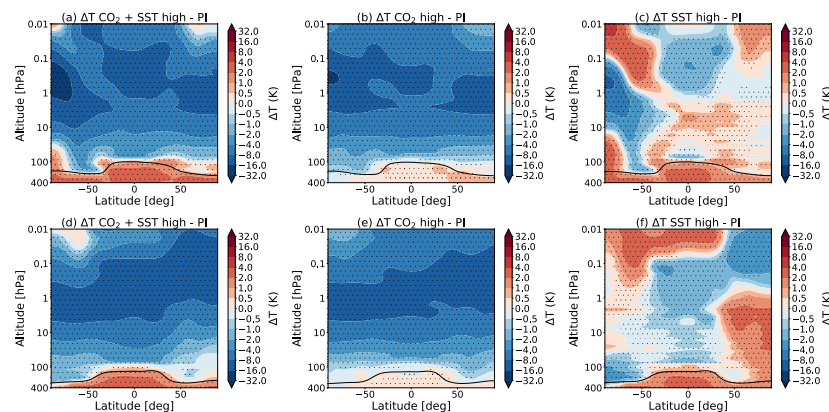445 *et al.,* 2007).

446

447
448 Figure 1: The total change in temperature in July (top) and January (bottom)
449 for (a,d) the simulation with high CO_2 and SSTs (S3), (b,e) the simulation with
450 high CO_2 (S1), (c,f) the simulation with high SSTs (S2), all as compared to the

9

pre-industrial control simulation (C1). The dotted regions indicate the regions where the data reaches a confidence level of 95%. The black line indicates the tropopause height for the experiments S3 (a,d), S1 (b,e) and S2 (c,f).

4. Meridional-vertical profiles of partial temperature changes

The CFRAM makes it possible to separate and estimate the temperature responses due to an external forcing and various climate feedbacks, such as ozone, water vapour, cloud, albedo and dynamical feedbacks. Note that for the ozone, water vapour, cloud and albedo feedback, we can only calculate the radiative part of the feedback. The response to dynamical changes is calculated in a separate term.

This can be understood as we use the Fu-Liou radiative transfer model (*Fu and Liou,* 1992, 1993) to do offline calculations of the total local thermal equilibrium (LTE) radiative heating rate perturbation fields between the control experiment C1 and one of the other three experiments (i.e, S1, or S2, or S3). We use the standard outputs of atmospheric compositions (e.g., CO_2 and O_3) and thermodynamic fields (e.g., pressure, temperature, water vapour, clouds, surface albedo) as well as partial LTE radiative heating rate perturbation fields due to perturbations in individual atmospheric composition or thermodynamic fields (e.g., the terms on the right hand side of (A.9) except the first term).

We use the difference between the offline calculation of the total LTE radiative heating rate perturbations and the original total LTE radiative heating rate perturbations derived directly from the standard WACCM outputs as the error term of our offline LTE radiative heating perturbations. We note that the standard WACCM output fields also include non-LTE radiative heating fields, but do not include non-radiative heating rates. Therefore, we use the sum of the total LTE radiative heating rate perturbations and non-LTE radiative heating fields derived from the standard WACCM output fields to infer non-radiative heating rate perturbations under the equilibrium condition, namely Eq. (A.8).

We should also note that, because we are using an atmosphere-only model, in our experiment, the external forcing is either the change in CO_2-concentration or the change in SSTs or both. In an atmosphere-ocean model (such as CESM) and, of course, in reality, the changes in sea surface temperature and sea ice distributions are responses to the changed CO_2-concentration.

In the following subsections 4.1-4.5, we will discuss the meridional-vertical profiles of the temperature responses to the direct forcing and the various feedbacks during July and January. In section 5, we will discuss regional and global means of partial temperature changes due to feedbacks.

4.1 Direct temperature response to CO_2

Figure 2 shows the zonal mean temperature change due to the increase in CO_2. We see that increasing CO_2 leads to a cooling almost everywhere in the

10

519 middle atmosphere, except at the high latitudes in the cold summer upper
520 mesosphere, where we see a warming instead. The higher the temperature,
521 the more cooling due to the increasing CO_2-concentration is found (*Shepherd,*
522 2008). The reason for this is that the outgoing longwave radiation strongly
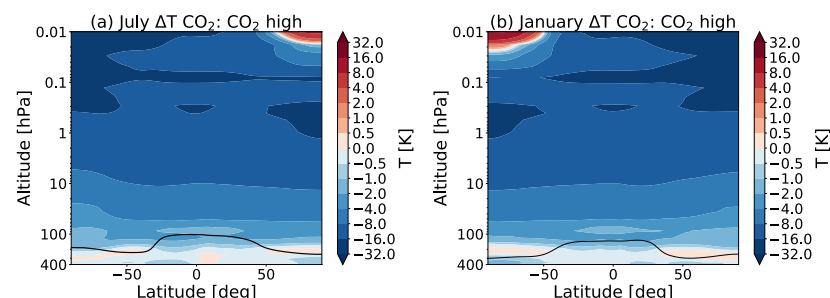523 depends on the Planck blackbody emission (*Zhu et al.,* 2016).
524

525
526 Figure 2: Partial temperature change due to the direct forcing of CO_2 for July
527 (top) and January (bottom) due to the doubling of the atmospheric CO_2-
528 concentration, as calculated by CFRAM, using experiment S1 and C1. The
529 black line indicates the tropopause height for the S1 run (with double CO_2-
530 concentration).
531
532 Changing the SSTs does not lead to a change in CO_2-concentration, therefore
533 the temperature response to changes in CO_2 is not present for the run with
534 only changed SST (Figures not shown).

4.2 Ozone feedback

536 Ozone plays a crucial role in the chemical and radiative budget of the middle
537 atmosphere. The distribution of ozone in the middle atmosphere is determined
538 by both chemical and dynamical processes. Most of the ozone production
539 takes place in the tropical stratosphere, as a result of photochemical
540 processes, which involve oxygen. Meridional circulation then transports ozone
541 to other parts of the middle atmosphere (*Langematz*, 2019). The production of
542 ozone is largely balanced by catalytic destruction cycles involving NO_x, HO_x
543 and Cl_x radicals. HO_x dominates ozone destruction in the mesosphere and
544 lower stratosphere, while NO_x and Cl_x dominate this process in the middle and
545 upper stratosphere (e.g. *Cariolle*, 1983).

546 Since the 1970s ozone in the middle atmosphere began to decline globally,
547 due to increased production of ozone depleting substances (ODSs) (*Brühl*
548 *and Crutzen*, 1988). The Montreal Protocol, adopted in 1987 to stop this
549 threat, eventually led to a slow recovery of the stratospheric ozone over the
550 recent two decades (*WMO*, 2018; *Langematz*, 2019). In our study, we don't
551 consider the effect of anthropogenic ODSs since pre-industrial times
552 (*Langematz*, 2019).

553 In this study, we are interested in the temperature response to changes in
554 ozone concentration induced by the increased CO_2 concentration and/or the

Deleted: C2

Deleted: C2 runs

11

557 changes in SST in WACCM. Under enhanced CO_2 concentrations, the ratio
558 between O_3 and O mixing ratios is generally shifted toward a higher
559 concentration of ozone, which is caused by the strong temperature
560 dependency of the ozone production reaction (O + O_2 + M $\rightarrow$ O_3 + M).

561 Fig. 3 shows the percentage changes in O_3-concentration when the CO_2-
562 concentration and/or the SSTs change. The results reach a statistical
563 significance of 95% for the whole middle atmosphere domain in the
564 experiments S3-C1 and S1-C1, and most of the middle atmosphere for
565 experiment S2-C1.
566
567 We find, as expected, that an increase in CO_2, leads to an increase of ozone
568 in most of the middle atmosphere. The increase of O_3 is about 20% around 2
569 hPa in the tropical region for experiment S3 with respect to C1. This
570 corresponds with what is seen by *Fomichev et al., (2007),* however they find
571 that the increase in ozone in January is a bit lower in this region (around 15%,
572 see their Figure 7).
573
574 There are some regions where the O_3-concentration is decreasing. In the
575 tropical lower stratosphere, a decrease of about 20% is seen, in the summer
576 polar mesosphere (around 0.01 hPa) ozone decreases by 3%, while in the
577 mesosphere (around 0.02 hPa), ozone decreases by over 30%. Fig. 3c and f
578 show that changing the SSTs also has a significant impact on the ozone
579 concentration. A complete account of the ozone changes is out of the scope
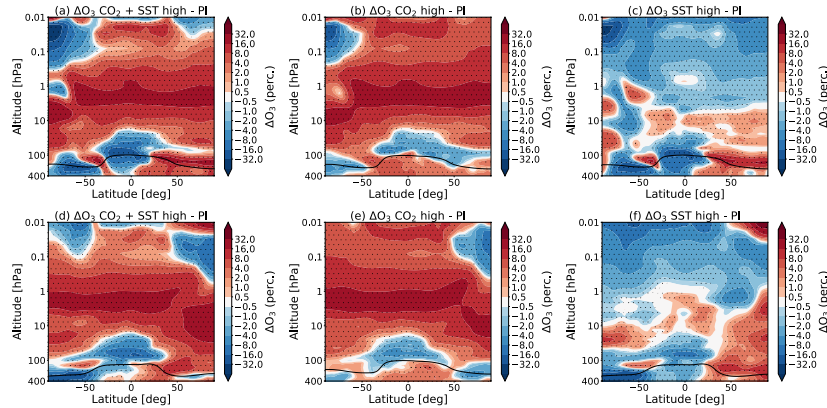580 of this paper.
581

582
583 Figure 3: The percentage change in the zonal and monthly mean ozone
584 concentration for July (top) and January (bottom) due to (a,d) combined effect
585 of the CO_2 increase and SSTs changes (experiments S3 -C1), (b,e) the
586 doubling of the atmospheric CO_2-concentration (experiments S1 - C1) and the
587 (c,f) SSTs (experiments S2 - C1), as simulated by WACCM. The dotted
588 regions indicate the regions where the data reaches a confidence level of
589 95%. The tropopause height is indicated as in Fig. 1.

597 As we will discuss in the next section, an enhanced concentration of CO_2 also
598 leads to changes in the dynamics in the middle atmosphere. The stratospheric
599 Brewer-Dobson circulation is projected to strengthen, which would lead to an
600 increase in the poleward transport of ozone. We will also see that an increase
601 in CO_2-concentration leads to stronger summer pole-to-winter pole flow in the
602 mesosphere.

603 Figure 4 shows the percentage change in the zonal and monthly mean
604 concentration of Cl, NO, O, OH, CH_3, NO_x and N_2O in July due to the
605 combined effect of the CO_2 increase and SSTs changes (experiment S3 vs
606 C1), as simulated by WACCM. The patterns in January look similar (not
607 shown). These results reach a statistical significance of 95% for the whole
608 middle atmosphere domain.

609 We would like to point out that the changes in these constituents are only
610 brought about by the CO_2-concentration and/or the SSTs. We still use the
611 F_1850 compset and the only difference between the runs is the forcing in
612 CO_2 and SSTs. The changes in chemical constituents look very similar to
613 those found by *Schmidt et al.* (2006) who performed a similar experiment as
614 discussed in section 2.2, see their Figure 20. Note that Fig. 4 shows the
615 changes due to both the CO_2 increase and SSTs changes, while their Figure
616 20 shows the percentage changes due to the changes in CO_2-concentration
617 only and also only above 1 hPa.

618 As in *Schmidt et al.* (2006), we see an decrease in atomic oxygen (O) mixing
619 ratio at high summer latitudes around 0.01 hPa (see Fig. 4c), which results
620 from increased upwelling. This increase in O leads to a decrease in ozone in
621 this region. We also see decrease of ozone concentration in the winter polar
622 region around 0.1 hPa (approximately 65 km). This could be caused by an
623 increase of NO and for a small part by Cl mixing ratios, which result from a
624 stronger subsidence of NO and Cl rich air, as suggested in Schmidt et al.
625 *2006*. As stated before, complete discussion of the changes in ozone
626 concentration is out of the scope of this paper and the changes in other
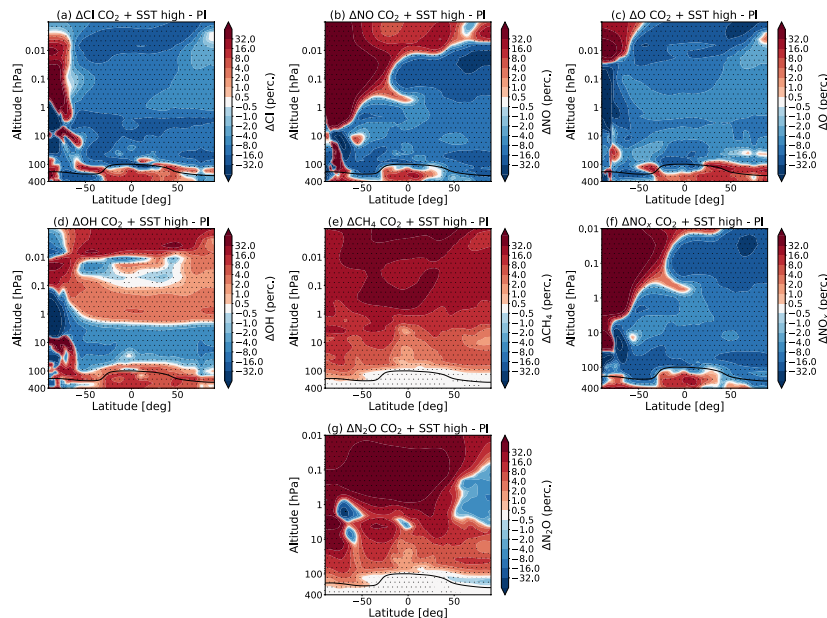627 constituents shown in Figure 4 are shown for reference only.

Deleted: S2

Figure 4: The percentage change in the zonal and monthly mean concentration of Cl (a), NO (b), O (c), OH (d), CH_4 (e) and NO_x (f) and N_2O (g) in July due to the combined effect of the CO_2 increase and SSTs changes (experiment (S3 vs C1), as simulated by WACCM. The dotted regions indicate the regions where the data reaches a confidence level of 95%. The tropopause height is indicated as in Fig. 1.

What is new in this study, is that we can calculate the temperature responses due to the changes in ozone concentration. These temperature responses are shown in Figure 5. It can be seen that there is a warming in the regions where there is an increase of the O_3-concentration, while there is a cooling for the regions with a decrease of the O_3-concentration. However, this is not the case for the winter polar region, where there is no sunlight. Note that the temperature responses to the changes in CO_2- and O_3- concentration behave differently in this respect: the temperature responses due to the direct forcing of CO_2 follow the temperature distribution quite closely, while the temperature responses due to O_3 follow the ozone concentration, as also seen by Zhu et al., *(2016).*
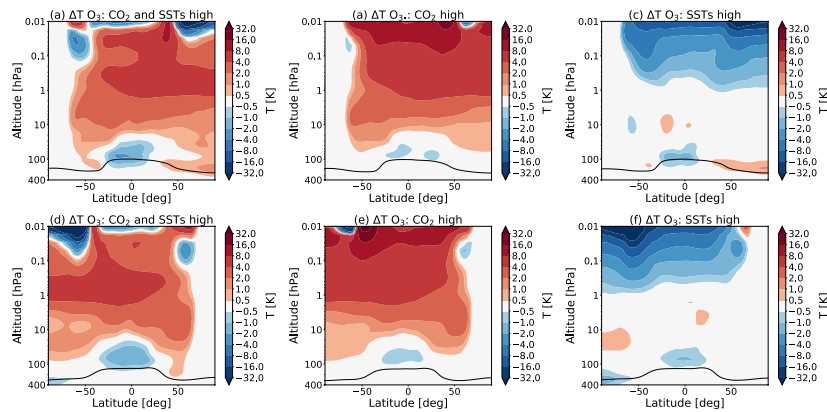
Figure 5: Partial temperature responses to changes in O_3-concentration, as calculated by CFRAM, in July (top) and January (bottom) due to the (a,d) combined effect of the CO_2 increase and SSTs changes (experiment S3), (b,e) the doubling of the atmospheric CO_2-concentration (experiment S1) and the (c,f) SSTs (experiment S2). The tropopause height is indicated as in Fig. 1.

4.2 Dynamical feedback

The zonal mean residual circulation forms an important component of the mass transport by the Brewer-Dobson circulation (BDC). It consists of a meridional (v^*) and a vertical (w^*) component as defined in the Transformed Eulerian Mean (TEM) framework. The residual circulation consists of a shallow branch, which controls the transport of air in the tropical lower stratosphere, as well as a deep branch in the mid-latitude upper stratosphere and mesosphere.

Both of these branches are driven by atmospheric waves. In the winter hemisphere, planetary Rossby waves propagate upwards into the stratosphere, where they break and deposit their momentum on the zonal mean flow, which in turns induces a meridional circulation. The two-cell structure in the lower stratosphere, which is present all-year round, is driven by synoptic scale waves. The circulation is also affected by orographic gravity wave drag in the stratosphere and by non-orographic gravity wave drag in the upper mesosphere (*Oberländer et al.*, 2013).

Most climate models show that the BDC and the upwelling in the equatorial region will speed up due to an increase in CO_2-concentration (*Butchart el al.,* 2010). It has been shown that the strengthening of the Brewer-Dobson circulation in the lower stratosphere is caused by changes in transient planetary and synoptic scale waves, while the upper stratospheric changes are due to changes in the propagation properties for gravity waves (*Oberländer et al.*, 2013).

684 It has been explained that the increased stratospheric resolved wave drag is
685 caused by an increase of the meridional temperature gradient in the
686 stratosphere, which leads to a strengthening of the upper flank of the
687 subtropical jets. This in turn shifts the critical layers for Rossby wave breaking
688 upward, which allows for more Rossby waves to reach the lower stratosphere,
689 where they break and deposit their momentum, enhancing the BDC
690 (*Shepherd and McLandress*, 2011)

691 The differences in the meridional component of the residual circulation (v^*)
692 between the different simulations are shown in Fig. 6. These data are
693 averaged over the 40 years of data. The results reach a statistical
694 significance of 95% almost the whole area above 1 hPa for the experiments
695 S1-C1, for the experiment S2-C1 the results reach a statistical significance of
696 95% in most of the area below this level. The experiments S3-C1 show the
697 largest region of statistical significance, apart from some regions below 1 hPa.

698 Figure 6b and 6e show that only doubling the CO_2-concentration leads to a
699 stronger pole-to-pole flow in the mesosphere. Changing the SSTs also leads
700 to changes in the residual circulation as can be seen in Fig. 6c and 6f.
701 Oberländer et al. (*2013*) have shown that the rising CO_2-concentration affects
702 the upper stratospheric layers, while the signals in the lower stratosphere are
703 almost completely due to changes in sea surface temperature.

704 The warmer sea surface temperatures affect the dynamics in the middle
705 atmosphere. It has for example been shown that higher SSTs in the tropics
706 leads to an amplification in deep convection, which enhances the generation
707 of quasi-stationary waves (*Deckert and Dameris, 2008*). Enhanced SSTs lead
708 to an enhanced dissipation of planetary waves, as well as an enhanced
709 dissipation of orographic and non-orographic waves in the upper stratosphere
710 (*Oberländer et al., 2013*).

711
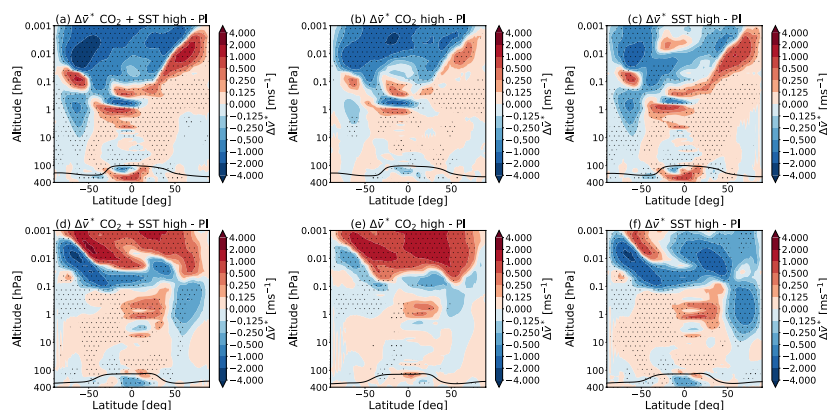
712
713 Figure 6: Changes in the zonal and monthly mean transformed Eulerian-mean
714 residual circulation horizontal velocity v^* for July (top) and January (bottom)
715 due to (a,d) combined effect of the CO_2 increase and SSTs changes

16

719 (experiments S3 -C1), (b,e) the doubling of the atmospheric CO_2-
720 concentration (experiments S1 - C1) and the (c,f) SSTs (experiments S2 -
721 C1), as simulated by WACCM. The dotted regions indicate the regions where
722 the data reaches a confidence level of 95%. The tropopause height is as
723 indicated in Fig. 1.

724 We are interested in the temperature responses due to the dynamical
725 feedbacks in the different experiments. These temperature responses are
726 shown in Figure 7. Figure 7b and 7e show that there is cooling in the summer
727 mesosphere, while there is warming in the winter mesosphere, which is
728 consistent with a stronger summer-to-winter pole flow.

729 Figure 7c and 7f show the temperature responses due to changes in the
730 SSTs. It is seen that there is mostly a warming in the summer mesosphere
731 and mostly a cooling in the winter hemisphere, which would weaken the effect
732 of the changed CO_2-concentration. Most of the temperature responses in the
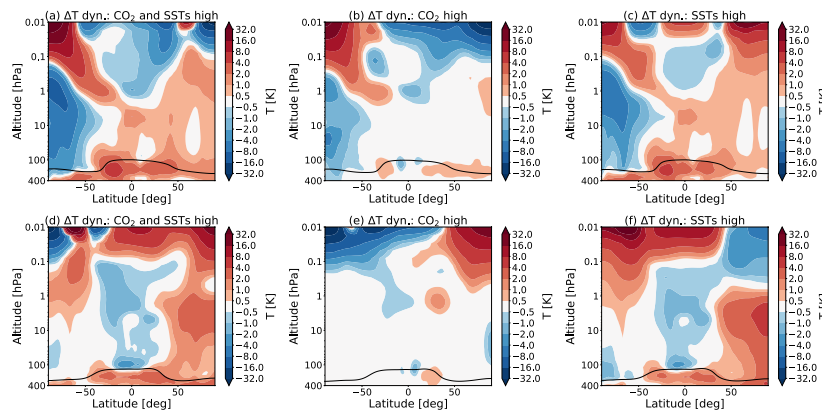733 lower stratosphere are caused by the changes in SSTs, as expected.

734

735 Figure 7: Partial temperature responses to changes in dynamics, as
736 calculated by CFRAM, in July (top) and January (bottom) due to the (a,d)
737 combined effect of the CO_2 increase and SSTs changes (experiment S3),
738 (b,e) the doubling of the atmospheric CO_2-concentration (experiment S1) and
739 the (c,f) SSTs (experiment S2). The tropopause height is indicated as in Fig.
740 1.

741 In summary, doubling the CO_2-concentration leads to a stronger pole-to-pole
742 flow in the mesosphere, which leads to cooling of the summer mesosphere
743 and a warming of the winter mesosphere. Changing the SSTs weakens this
744 effect, but leads to temperature changes in the stratosphere and lower
745 mesosphere.

746 **4.4 Water vapour feedback**
747

754 Figure 8 shows how the water vapour is changing in the middle atmosphere if
755 the CO_2-concentration is increased and/or the SSTs are changed with respect
756 to the pre-industrial control run. In WACCM, increasing the CO_2-concentration
757 alone leads to a decrease of water vapour in most of the middle atmosphere
758 (Fig. 8b and f). The results reach a statistical significance of 95% for the
759 whole middle atmosphere domain in the experiments S3-C1 and S2-C1, and
760 most of the middle atmosphere for experiment S1-C1, apart from the winter
761 hemisphere region around 0.1 hPa.
762
763 The amount of water vapour in the stratosphere is determined by transport
764 through the tropopause as well as by the oxidation of methane in the
765 stratosphere itself. The transport of the water vapour in the stratosphere is
766 mainly a function of the tropopause temperature (*Solomon et al.,* 2010). In
767 WACCM, we see a decrease in temperature in the tropical tropopause for the
768 double CO_2 experiment of about -0.25 K. The cold temperatures in the tropical
769 tropopause lead to a reduction of water vapour of between 2 and 8% due to
770 freeze-drying in this region.
771
772 It can be seen that using the SSTs from the doubled CO_2-climate leads to an
773 increase in water vapour almost everywhere in the middle atmosphere as
774 compared to PI (Fig. 8c and f). In WACCM, forcing with SSTs from a double
775 CO_2-climate is observed to lead to a higher and warmer tropopause, which
776 can explain this increase of water vapour. However, it should be noted that
777 models currently have a limited representation of the processes determining
778 the distribution and variability of lower stratospheric water vapour. Minimum
779 tropopause temperatures are not consistently reproduced by climate models
780 (*Solomon et al.,* 2010; *Riese et al.,* 2012). At the same time, observations are
781 not completely clear about whether there is a persistent positive correlation
782 between the SST and the stratospheric water vapour (*Solomon et al.*, 2010).
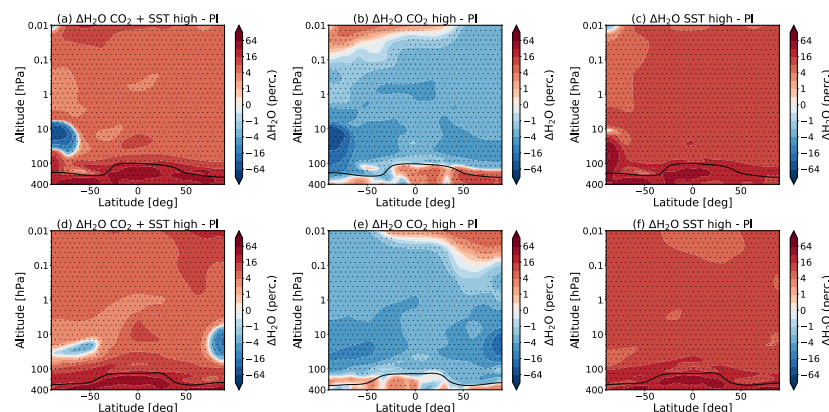783

784
785 Figure 8: The percentage changes in the zonal and monthly mean water
786 vapour mixing ratio for July (top) and January (bottom) due to (a,d) combined
787 effect of the CO_2 increase and SSTs changes (experiments S3 - C1), (b,e) the
788 doubling of the atmospheric CO_2-concentration (experiments S1 - C1) and the
789 (c,f) SSTs (experiments S2 - C1), as simulated by WACCM. The dotted

796 regions indicate the regions where the data reaches a confidence level of
797 95%. The tropopause height is as indicated in Fig. 1.
798
799 Figure 9 shows the temperature responses due to the changes in water
800 vapour as calculated by CFRAM. It can be seen that in the regions where
801 there is an increase in the water vapour, there is a cooling, and vice versa.
802 This can be understood as increasing the water vapour in the middle
803 atmosphere leads to an increase in longwave emissions in the mid and far-
804 infrared by water vapour. This in turns leads to a cooling of the region.
805 Similarly, a decrease in water vapour leads to a warming of the region
806 (*Brasseur and Solomon,* 2005). Fig. 8 shows that above 1 hPa, there are also
807 large percentage changes in water vapour. However, the absolute
808 concentration of water vapour is small there, which explains why there is no
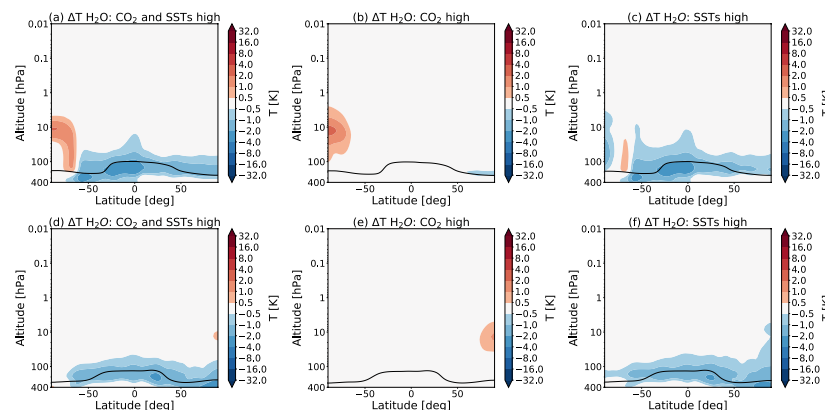809 temperature response to these changes.
810

811
812 Figure 9: Partial temperature responses to changes in water vapour, as
813 calculated by CFRAM, in July (top) and January (bottom) due to the (a,d)
814 combined effect of the CO_2 increase and SSTs changes (experiment S3),
815 (b,e) the doubling of the atmospheric CO_2-concentration (experiment S1) and
816 the (c,f) SSTs (experiment S2). The tropopause height is indicated as in Fig.
817 1.

818
819 Water vapour plays a secondary but not negligible role in determining the
820 middle atmosphere climate sensitivity. In the lower stratosphere, H_2O
821 contributes considerably to the cooling in this region. Above 30 hPa, the water
822 vapour contribution to the energy budget is negligible, as also seen by
823 *Fomichev et al.* (2007).
824
825 **4.5 Cloud and albedo feedback**
826
827 Forcing the model with SSTs from the double CO_2-climate (as in experiment
828 S2 and S3) yields an overall increase in the cloud cover in the upper
829 troposphere, while this is not the case if one only increases the CO_2
830 concentration (as in experiment S1). Figure 10 shows the temperature

19

838 responses to changes in cloud (left) and albedo (right) in July (top) and
839 January (bottom) for experiment S2, as calculated by CFRAM.

840
841 Fig. 10 shows in the tropical region, there is a warming due to changes in
842 clouds, while there is a cooling at higher latitudes in July (see Figure 10a). In
843 January, the pattern looks slightly different (see Figure 10c). These
844 temperature changes are due to changes in the balance between the
845 increased reflected shortwave radiation and the decrease of outgoing
846 longwave radiation.
847
848 We also see an effect of the changes in surface albedo in the stratosphere
849 (see Figure 10b and d). The cooling in the summer polar stratosphere shown
850 in Figure 10b and d is due to radiative changes. We suggest that this cooling
851 is due to a decrease in surface albedo, which would lead to less shortwave
852 radiation being reflected. However, more research is needed.
853
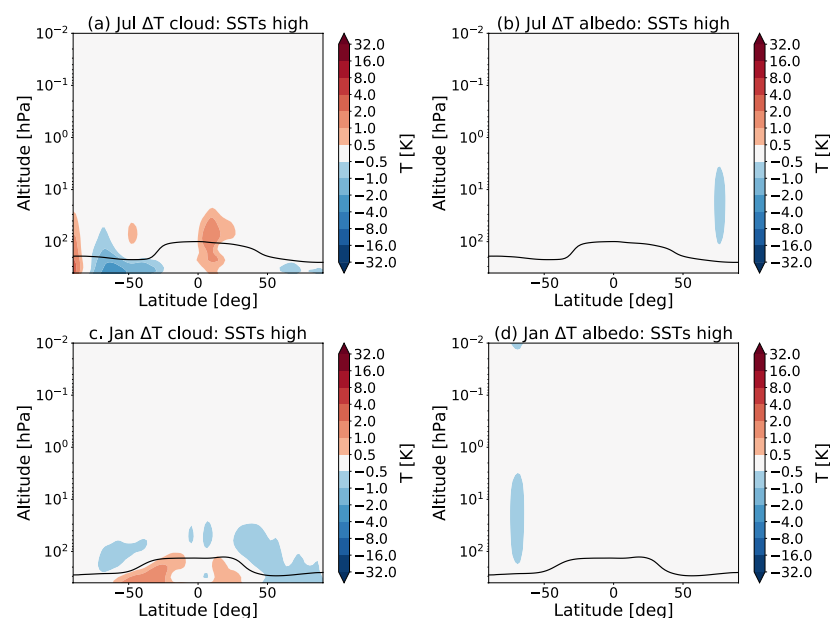
854
855 Figure 10: Partial temperature responses to changes in clouds (left) and
856 albedo (right), as calculated by CFRAM, in July (top) and January (bottom)
857 due to the SSTs (experiment S2). The tropopause height is indicated as in
858 Fig. 1.

859
860 Cloud and albedo feedbacks due to changes in clouds and surface albedo
861 play a crucial role in determining the tropospheric and surface climate
862 (*Boucher et al.,* 2013, *Royer et al.,* 1990). However, it is clear that these
863 feedbacks play only a very small role in the middle atmosphere temperature
864 response to the doubling of CO_2 and SSTs.
865

5. Regional and global means of partial temperature changes due to feedbacks

To study the relative importance of the different feedback processes globally we show the average change in global mean temperature for the lower stratosphere, the upper stratosphere and the mesosphere for the S3 experiment with the changed CO_2-concentration and changed SSTs in Figure 11. We also show the average change in temperature in the polar regions (90°S-70°S and 70°N-90°N), the tropics (20°S-20°N) for the lower and upper stratosphere and the mesosphere.

In order to calculate the lower stratospheric temperature changes, we take the average value of the temperature change from the tropopause up to 24 hPa. The pressure level of the tropopause is simulated in WACCM for each latitude and longitude, we use this pressure level to demarcate between the troposphere and stratosphere. We consider 24 hPa as a crude estimate for the boundary between the lower and upper stratosphere.

The tropopause is not exactly at the same pressure level in the perturbation experiments as compared to the pre-industrial control run (C1). We always take the tropopause of the perturbation experiment which is a bit higher at some latitudes, to make sure that we do not use values from the troposphere. We add the values for each latitude up and take the average. This average is not mass weighted. By calculating the average in this way, we can directly compare the vertical values in different regions of the atmosphere. The temperature changes in the upper stratosphere and in the mesosphere are calculated in the same way, but then for the altitudes 24 hPa-1 hPa and 1 hPa-0.01 hPa respectively.

Figure 11 shows the radiative feedbacks due to ozone, water vapour, clouds, albedo and the dynamical feedback, as well as the small contribution due to the Non-LTE processes in column 'NLTE', as calculated by CFRAM. The 'total'-column shows the temperature changes in WACCM, while the column 'error' shows the difference between temperature change in WACCM and the sum of the calculated temperature responses in CFRAM. Note that the range of values on the y-axis is not the same for the different subplots.

Figure 11 shows that the temperature change in the lower stratosphere due to the direct forcing of CO_2 is around 3 K in the global mean. There is a stronger cooling in the tropical region of about 4 K in July and 3.5 K in January. We also observe that there is a cooling of about 1 K due to ozone feedback in the tropical region while there is a slight warming taking place in the summer hemispheres in both January and July. We also see that the temperature change in the lower stratosphere is influenced by the water vapour feedback. There is a cooling of about 0.5 K in the lower stratosphere, apart from in the southern polar area. There is some small influence from the cloud and albedo feedback, which can be negative or positive (see also Fig. 9).

In the upper stratosphere, the cooling due to the direct forcing of CO_2 is with about 9 K in the global mean considerably stronger than in the lower

Deleted: S2

Deleted: stratosphere

Deleted: until

Deleted: taking

21

922 stratosphere. The cooling is stronger in the summer polar regions, where the
923 cooling due to the direct forcing of CO_2 reaches 11K. In the winter polar
924 region, this cooling is only about 8K.
925
926 The water vapour, cloud and albedo feedback play no role in the upper
927 stratosphere nor in the mesosphere. The ozone feedback results in the
928 positive partial temperature changes in the upper stratosphere, of about 2 K in
929 the global mean. The changes in ozone don't result in temperature changes in
930 the winter hemisphere, as discussed in section 4.2.
931
932 The picture in the mesosphere is similar as in the upper stratosphere. The
933 main difference is that the temperature changes are larger. The global
934 temperature change due to direct forcing of CO_2 is about 15 K. The O_3-
935 feedback results in a partial temperature changes of about 3 K in the
936 mesosphere in the global mean. The temperature change due to ozone in the
937 equatorial mesosphere is about 4 K, while the warming due to ozone in the
938 summer polar region is a bit smaller: around 3K. Just like in the upper
939 stratosphere water vapour, cloud and albedo feedback play no role.
940
941 We see, that the ozone feedback generally yields a radiative feedback that
942 mitigates the cooling, which is due to the direct forcing of CO_2. This has been
943 suggested in earlier studies, such as *Jonsson et al., 2004, Dietmüller et al.,*
944 *2014*. With CFRAM, it is possible to quantify this effect and to compare it with
945 the effects of other feedbacks in the middle atmosphere. Note that no other
946 method before has been able to quantify how much of the temperature
947 change in the middle atmosphere is due to the different feedback processes.
948
949 The temperature response due to dynamical feedbacks is small in global
950 average: less than 1 K. This can be understood as waves generally do not
951 generate momentum and heat, but redistribute these instead (*Zhu et al.,*
952 2016). However, the local responses to dynamical changes in the high
953 latitudes are large, as we have seen in section 4.2. There are some very small
954 temperature responses due to non-LTE effects as well, which mostly
955 contribute to the temperature change in the mesosphere.
956
957 The error term is relatively large, as can be seen from the rightmost column in
958 Fig.11. This term shows the difference between temperature change in
959 WACCM and the sum of the calculated temperature responses in CFRAM
960 (see eq. 9 in section 2.3). In CFRAM, we assumed that the radiative
961 perturbations can be linearized by neglecting the higher order terms of each
962 thermodynamic feedback and the interactions between these feedbacks, this
963 yields an error.
964
965 Cai and Lu (*2009*) show that this error is larger in the middle atmosphere than
966 for similar calculations in the troposphere. In the middle atmosphere, the
967 density of the atmosphere is smaller, which leads to smaller numerical values
968 of the diagonal elements of the Planck feedback matrix. As a result, the linear
969 solution is very sensitive to forcing in the middle atmosphere. Another part of
970 the error is due to the fact that the radiative transfer model used in the offline

Deleted: before

Deleted: mostly

Deleted: The error term is relatively large.

Formatted: Font: 12 pt

Formatted: Font: 12 pt

Formatted: x_body, Line spacing: At least 12,65 pt, Widow/Orphan control, Adjust space between Latin and Asian text, Adjust space between Asian text and numbers

22

974 CFRAM calculations is different than the radiative transfer model used in the
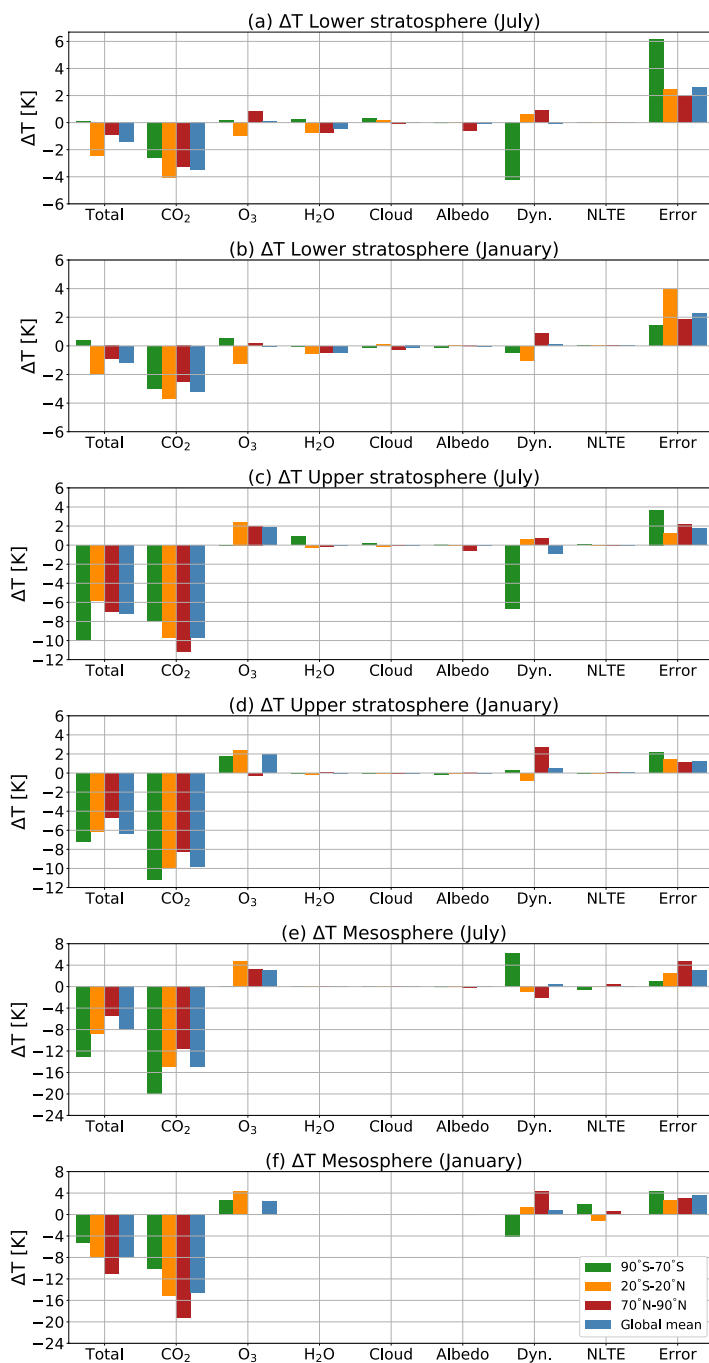975 climate simulations with WACCM.
976

(a) ΔT Lower stratosphere (July)

(b) ΔT Lower stratosphere (January)

(c) ΔT Upper stratosphere (July)

(d) ΔT Upper stratosphere (January)

(e) ΔT Mesosphere (July)

(f) ΔT Mesosphere (January)

977

978   Figure 11: The mean temperature responses to the changes in CO_2 and
979   various feedback processes in the lower stratosphere from the tropopause
980   height up to 24 hPa (a,b), upper stratosphere from 24-1 hPa (c, d) and in the
981   mesosphere from 1-0.01 hPa (e,f) in July (a, c, e) and January (b, d, f) in the
982   polar regions (90°S-70°S and 70°N-90°N), the tropics (20°S-20°N) and the
983   global mean, for S3 experiment (double CO_2 and changed SSTs). Note that
984   the range of values on the y-axis is not the same for the different subplots.
985
986   In addition, the vertical profiles of the temperature responses to the direct
987   forcing of CO_2 and the feedbacks are shown in Figure 12. Here, one can see
988   that the increase in CO_2 leads to a cooling over almost the whole middle
989   atmosphere; an effect that increases with height. We also observe that in the
990   summer upper mesosphere regions, the increased CO_2-concentration leads
991   to a warming. The changes in ozone concentration in response to the
992   doubling of CO_2 lead to a warming almost everywhere in the atmosphere. In
993   some places, this warming exceeds 5 K. In the polar winter the effect of ozone
994   is small due to lack of sunlight.
995
996   There is also a relatively large temperature response to the changes in
997   dynamics. In Fig. 12, it can be seen that there is a cooling in the summer
998   mesosphere, while there is warming in the winter mesosphere. The water
999   vapour, cloud and albedo feedback play only a very small role in the middle
1000   atmosphere, as we observed in Figure 11. We find that there are also some
1001   small temperature changes due to non-LTE effect above 0.1 hPa. How the
1002   non-LTE effects exactly cause the small temperature changes in this region is
1003   outside the scope of this paper and needs further investigation.
1004

Temperature responses to different feedback processes

1005
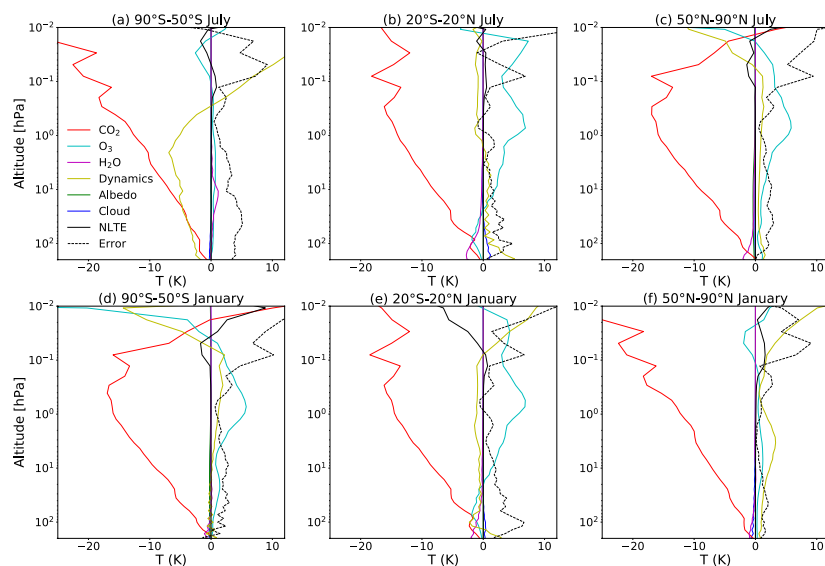
Deleted: until

Deleted: S1

Deleted: The Non-LTE effects

Deleted: , but start

Deleted: play a small role

Deleted: ,

Deleted: exact mechanism of which

1013 Figure 12: Vertical profiles of the temperature responses to the changes in
1014 CO_2 and various feedback processes in July (top) and January (bottom) due
1015 to double CO_2 and changed SSTs in the atmosphere between 200 and 0.01
1016 hPa, for regions from 50° N/S poleward and the tropics (20°S-20°N), as
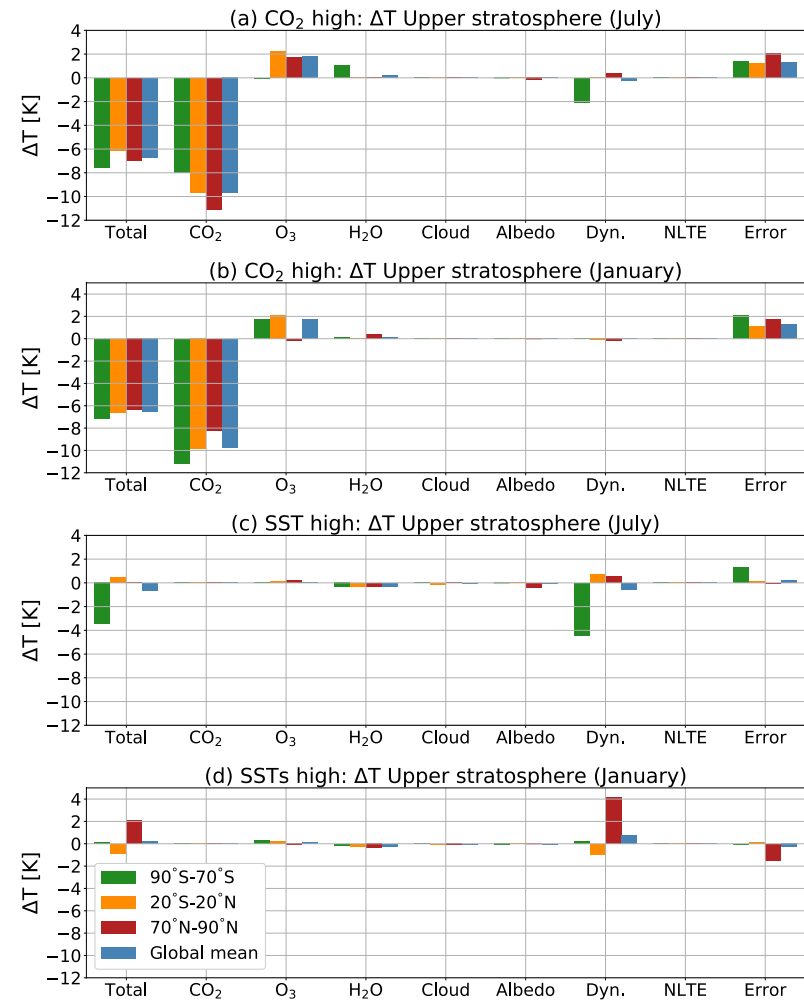1017 calculated by CFRAM.
1018

(a) CO_2 high: ΔT Upper stratosphere (July)

(b) CO_2 high: ΔT Upper stratosphere (January)

(c) SST high: ΔT Upper stratosphere (July)

(d) SSTs high: ΔT Upper stratosphere (January)

1019
1020 Figure 13: The mean temperature responses to the changes in CO_2 and
1021 various feedback processes in July (a,c) and January (b,d) in the upper
1022 stratosphere between 24 and 1 hPa, for polar regions (90°S-70°S and 70°N-
1023 90°N), the tropics (20°S-20°N) and the global mean for the experiment with
1024 double CO_2 (S1) (a,b) and changed SSTs (S2) (c,d) separately.
1025

26

1029

1030 Figure 13 shows the temperature responses in the upper stratosphere for the
1031 experiment with double CO_2 (a,b) and changed SSTs (c,d) separately. This
1032 has been done to give insight in the temperature response of the CO_2 and the
1033 SST separately. These temperature changes were calculated in the same
1034 way as for Fig. 11. Again also, the 'total'-column shows the temperature
1035 changes as simulated by WACCM, the columns CO_2, O_3, H_2O, cloud, albedo,
1036 dynamics, the column 'NLTE' shows the temperature responses due to non-
1037 LTE processes as calculated by CFRAM. As in Fig. 11, the 'Error'-column in
1038 Fig.13 shows the difference between temperature change in WACCM and the
1039 sum of the calculated temperature responses in CFRAM.
1040

1041 We learn from this figure that the effects of the changed SSTs on the upper
1042 stratosphere are relatively small as compared to the effects of changing the
1043 CO_2. We show the temperature changes for the upper stratosphere as an
1044 example. In the lower stratosphere and the mesosphere, we see the same
1045 pattern: the effect of the CO_2 on the temperature is generally much larger than
1046 the effect of the SSTs on the temperature. This finding is consistent with the
1047 study of *Fomichev et al.* (2007), where it is concluded that the impact of
1048 changes in SSTs on the middle atmosphere is relatively small and localized
1049 as compared to the combined response of changing the CO_2-concentration
1050 and the SSTs.
1051

1052 The changes in SSTs are, however, responsible for large temperature
1053 changes as a result of the dynamical feedbacks, especially in the winter
1054 hemispheres, where there is a temperature response of 4K. A similar figure
1055 for the lower stratosphere (not shown) shows that the temperature response
1056 to the water vapour feedback is almost solely due to changes in the SSTs and
1057 not the direct forcing of CO_2.
1058

1059 Earlier, we discussed that the sum of the two separate temperature changes
1060 in the experiment with double CO_2 and changed SSTs is approximately equal
1061 to the changes observed in the combined simulation. We find that the same is
1062 true for the temperature responses to the different feedback processes.
1063

1064 **5. Discussion and conclusions**
1065

1066 In this study, we have applied the climate feedback response analysis method
1067 to climate sensitivity experiments performed by WACCM. We have examined
1068 the middle atmosphere response to CO_2 doubling with respect to the pre-
1069 industrial state. We investigated the combined effect of doubling CO_2 and
1070 subsequent warming SSTs, as well as the effects of separately changing the
1071 CO_2 and the SSTs. It is important to note that no other method before has
1072 been able to quantify how much of the temperature change in the middle
1073 atmosphere is due to the different feedback processes.
1074

1075 It was found before that the sum of the two separate temperature changes in
1076 the experiment with only changed CO_2 and only changed SSTs is, at first
1077 approximation, equal to the changes observed in the combined simulation

Deleted: ¶
¶

Deleted: on-

Deleted: LTE

Deleted: Error

Deleted: before

27

1084 (see e.g. *Fomichev et al. (2007) and Schmidt et al. (2006)*). This is also the
1085 case for WACCM.
1086
1087 We have found that, even though changing the SSTs yields significant
1088 temperature changes over a large part of the middle atmosphere, the effects
1089 of the changed SSTs on the middle atmosphere are relatively small as
1090 compared to the effects of changing the CO_2 without changes in the SSTs.

1091 We have given an overview of the mean temperature responses to the
1092 changes in CO_2 and various feedback processes in the lower stratosphere,
1093 upper stratosphere and in the mesosphere in January and July. We find that
1094 the temperature change due to the direct forcing of CO_2 increases with
1095 increasing height in the middle atmosphere. The temperature change in the
1096 lower stratosphere due to the direct forcing of CO_2 is around 3 K. There is a
1097 stronger cooling in the tropical lower stratosphere of about 4 K in July and 3.5
1098 K in January.

1099 In the upper stratosphere, the cooling due to the direct forcing of CO_2 is about
1100 9 K, which is considerably stronger than in the lower stratosphere. The
1101 cooling is stronger in the summer polar regions, where the cooling reaches a
1102 value of 11K, than in the winter polar region, where the cooling is only about
1103 8K. In the mesosphere, the cooling due to the direct forcing of CO_2 is even
1104 stronger: 15 K.

1105 The ozone concentration changes due to changes in the CO_2-concentration
1106 as well as by changes in the SSTs. The temperature changes caused by this
1107 change in ozone concentration generally mitigate the cooling caused by the
1108 direct forcing of CO_2. However, in the tropical lower stratosphere and in some
1109 regions of the mesosphere, the ozone feedback cools these regions further. In
1110 the tropical lower stratosphere, for example, there is a cooling of 1K due to
1111 the ozone feedback.
1112
1113 We also have seen that the global mean temperature response due to
1114 dynamical feedbacks is small in the global average in all regions: less than 1
1115 K. However, local responses to the changes in dynamics can be large.
1116 Doubling the CO_2-concentration leads to a stronger summer-to-winter-pole
1117 flow, which leads to a cooling of the summer mesosphere and a warming of
1118 the winter mesosphere. Changing the SSTs weakens this effect in the
1119 mesosphere, but affects the temperature response in the stratosphere and
1120 lower mesosphere.
1121
1122 Using CFRAM on WACCM data shows that the change in water vapour leads
1123 to a cooling of up to 2 K in the lower stratosphere. It should be noted that
1124 climate models currently have a limited representation of the processes
1125 determining the distribution and variability of lower stratospheric water vapour.
1126 This means that the temperature response to the water vapour feedback
1127 might be different using a different model. We have also seen a small effect of
1128 the cloud and albedo feedback on the temperature response in the lower
1129 stratosphere, while these feedbacks play no role in the upper stratosphere
1130 and the mesosphere.

28

1132
1133 The results seen in this study are consistent with earlier findings. As in
1134 *Shepherd et al*., (2008), we find that the higher the temperature at a region in
1135 the atmosphere, the more cooling there is seen due to the direct feedback of
1136 CO_2. We find, as in *Zhu et al*., (2016) that the temperature responses due to
1137 the direct forcing of CO_2 follow the temperature distribution quite closely, while
1138 the temperature responses due to O_3 follow the changes in ozone
1139 concentration instead.
1140
1141 We have also seen that the ozone feedback generally yields a radiative
1142 feedback that mitigates the cooling, which is due to the direct forcing of CO_2,
1143 which is consistent with earlier studies such as *Jonsson et al., (2004),*
1144 *Dietmüller et al., (2014)*. CFRAM is the first study that allows for calculating
1145 how much of the temperature response is due to which feedback process.
1146
1147 The next step would be to investigate the exact mechanisms behind the
1148 feedback processes in more detail. Some processes can influence the
1149 different feedback processes, such as ozone depleting chemicals influencing
1150 the ozone concentration and thereby the temperature response of this
1151 feedback. A better understanding of the effect of the increased CO_2-
1152 concentration on the middle atmosphere, will help to distinguish the effects of
1153 the changes CO_2- and O_3-concentration.
1154
1155 There is also a need for a better understanding of how different feedbacks in
1156 the middle atmosphere affect the surface climate. As discussed in the
1157 introduction, the exact importance of ozone feedback on the global mean
1158 temperature is currently not clear (*Nowack et al*., 2015, *Marsh et al.*, 2016). A
1159 similar analysis as in this paper can be performed to quantify the effects of
1160 feedbacks on the surface climate.
1161
1162 In conclusion, we have seen that CFRAM is an efficient method to quantify
1163 climate feedbacks in the middle atmosphere, although there is a relatively
1164 large error due to the linearization in the model. The CFRAM allows for
1165 separating and estimating the temperature responses due to an external
1166 forcing and various climate feedbacks, such as ozone, water vapour, cloud,
1167 albedo and dynamical feedbacks. More research into the exact mechanisms
1168 of these feedbacks could help us to understand the temperature response of
1169 the middle atmosphere and their effects on the surface and tropospheric
1170 climate better.
1171
1172 **Appendix: Formulation of CFRAM diagnostics using outputs of WACCM**
1173
1174 The mathematical formulation of CFRAM is based on the conservation of total
1175 energy (*Lu and Cai*, 2009). At a given location in the atmosphere, the energy
1176 balance in an atmosphere-surface column can be written as:
1177
1178 $R = S + Q^{conv} + Q^{turb} - D^v - D^h + W^{fric}$ (A1)
1179
1180 R represents the vertical profile of the net long-wave radiation emitted by each
1181 layer in the atmosphere and by the surface. S is the vertical profile of the solar

1182 radiation absorbed by each layer. Q^{turb} is the convergence of total energy
1183 fluxes in each layer due to turbulent motions, Q^{conv} is convergence of total
1184 energy fluxes into the layers due to convective motion. D^v is the large-scale
1185 vertical transport of energy from different layers to others. D^h is the large-
1186 scale horizontal transport within the layers and W^{fric} is the work done by
1187 atmospheric friction. All terms in (A1) have units of Wm^{-2}.
1188
1189 Due to an external forcing (in this study, the change in CO_2-concentration
1190 and/or change in SSTs), the difference in the energy flux terms then
1191 becomes:
1192
1193 $\Delta R = \Delta F^{ext} + \Delta S + \Delta Q^{conv} + \Delta Q^{turb} - \Delta D^v - \Delta D^h + \Delta W^{fric}$ (A2)
1194
1195 In which the delta (Δ) stands for the difference between the perturbation run
1196 and the control run.
1197
1198 CFRAM takes advantage of the fact that the infrared radiation is directly
1199 related to the temperatures in the entire column. The temperature changes in
1200 the equilibrium response to perturbations in the energy flux terms can be
1201 calculated. This is done by requiring that the temperature-induced changes in
1202 infrared radiation balance the non-temperature induced energy flux
1203 perturbations.
1204
1205 Equation (A2) can also be written as:
1206
1207 $\Delta(S - R)_{total} + \Delta dyn = 0$ (A3)
1208
1209 The term $\Delta(S - R)$ can be calculated as the longwave heating rate and the
1210 solar heating rate are output variables of the model simulations. We take the
1211 time mean of the WACCM data and perform the calculations for each grid
1212 point of the WACCM data. This means that in the end, we will have the
1213 temperature changes at each latitude, longitude and height.
1214
1215 We then calculate the difference in these heating rates for the perturbation
1216 simulation and the control simulation.
1217
1218 We use the term $\Delta(S - R)_{total}$ to calculate the dynamics term Δdyn.
1219
1220 $\Delta dyn = -\Delta(S - R)_{total}$ (A4)
1221
1222 WACCM provides us with a heating rate in Ks^{-1}. For the CFRAM calculations,
1223 we need the energy flux in Wm^{-2}. We can calculate the energy flux by
1224 multiplying with the mass of different layers in the atmosphere and the specific
1225 heat capacity.
1226
1227 $\Delta(S - R) = \Delta(S - R)_{(WACCM)} * mass_k * c_p$ (A5)
1228

1229 In which $\Delta(S - R)$ is the difference in the shortwave radiation (S) and
1230 longwave radiation (R) between the perturbation run and the control run as a
1231 flux in Wm^{-2}, while $\Delta(S - R)_{(WACCM)}$ is this difference as heating rate in Ks^{-1} in
1232 WACCM, with $mass_k = \frac{p_{k+1} - p_k}{g}$ with p in Pa, $c_p = 1004$ J kg^{-1} K^{-1} the
1233 specific heat capacity at constant pressure and g the gravitational
1234 acceleration 9.81 ms^{-2}.
1235
1236 WACCM includes a non-local thermal equilibrium (non-LTE) radiation scheme
1237 above 50 km. It consists of a long-wave radiation (LW) part and a short-wave
1238 radiation (SW) part which includes the extreme ultraviolet (EUV) heating rate,
1239 chemical potential heating rate, CO_2 near-infrared (NIR) heating rate, total
1240 auroral heating rate and non-EUV photolysis heating rate.
1241 Therefore, we split the term $\Delta(S - R)_{total}$ in an LTE and a non-LTE term:
1242
1243 $$\Delta(S - R)_{total} = \Delta(S - R)_{LTE} + \Delta(S - R)_{non-LTE} \qquad \text{(A6)}$$
1244
1245 WACCM provides us with the total longwave heating rate as well as the total
1246 solar heating rate and the non-LTE longwave and shortwave heating rates for
1247 the different runs. This means that we can calculate the term $\Delta(S - R)_{non-LTE}$
1248 as well, where we again need to convert our result from Ks^{-1} to Wm^{-2}:
1249
1250 $$\Delta(S - R)_{non-LTE} = \Delta(S - R)_{non-LTE(WACCM)} \ mass_k * c_p \qquad \text{(A7)}$$
1251
1252 This term can be inserted in equation (3):
1253
1254 $$\Delta(S - R)_{LTE} + \Delta(S - R)_{non-LTE} + \Delta dyn = 0 \qquad \text{(A8)}$$
1255
1256 The central step in CFRAM is to decompose the radiative flux vector, using a
1257 linear approximation.
1258
1259 We start by decomposing the LTE infrared radiative flux vector ΔR
1260
1261 $$\Delta R_{LTE} = \frac{\partial R}{\partial T}\Delta T + \Delta R_{CO_2} + \Delta R_{O_3} + \Delta R_{H_2O} + \Delta R_{albedo} + \Delta R_{cloud} \qquad \text{(A9)}$$
1262
1263 where ΔR_{CO_2} , ΔR_{O_3} , ΔR_{H_2O} , ΔR_{albedo} , ΔR_{cloud} are the changes in infrared
1264 radiative fluxes due to the changes in CO_2, ozone, water vapour, albedo and
1265 clouds, respectively.
1266
1267 For equation (A9), we assumed that radiative perturbations can be linearized
1268 by neglecting the higher order terms of each thermodynamic feedback and
1269 the interactions between these feedbacks. This is also commonly done in the
1270 partial radiative perturbation (PRP) method, in which partial derivatives of the
1271 model top of the atmosphere radiation are evaluated with respect to changes
1272 in model parameters by diagnostic rerunning the model's radiation code (*Bony*
1273 *et al.,* 2006).
1274

1275 The term $\frac{\partial R}{\partial T}\Delta T$ represents the changes in the IR radiative fluxes related to the

1276 temperature changes in the entire atmosphere-surface column. The matrix $\frac{\partial R}{\partial T}$

1277 is the Planck feedback matrix, in which the vertical profiles of the changes in
1278 the divergence of radiative energy fluxes due to a temperature change are
1279 represented.
1280
1281 We calculate this feedback matrix using the output variables of the
1282 perturbation and the control run of WACCM and inserting these in the CFRAM
1283 radiation code: atmospheric temperature, surface temperature, reference
1284 height temperature, ozone, surface pressure, solar insolation, downwelling
1285 solar flux at the surface, net solar flux at the surface, dew point temperature,
1286 cloud fraction, cloud ice amount, cloud liquid amount, ozone and specific
1287 humidity.
1288
1289 Similarly, the changes in the LTE shortwave radiation flux can be written as
1290 the sum of the change in shortwave radiation flux due to the direct forcing of
1291 CO_2 and the different feedbacks:
1292
1293 $\Delta S_{LTE} = \Delta S_{CO_2} + \Delta S_{O_3} + \Delta S_{H_2O} + \Delta S_{albedo} + \Delta S_{cloud}$ (A10)

1294
1295 Similarly, to equation (A9), we perform a linearization.
1296
1297 Substituting (A9) and (A10) in equation (A8) yields:
1298

1299 $\Delta(S-R)_{CO_2} + \Delta(S-R)_{O_3} + \Delta(S-R)_{H_2O} + \Delta(S-R)_{albedo} + \Delta(S-R)_{cloud} - \frac{\partial R}{\partial T}\Delta T$

1300 $+\Delta(S-R)_{non-LTE} + \Delta dyn = 0$ (A11)

1301
1302 This can be written as:
1303

1304 $\Delta T = \left(\frac{\partial R}{\partial T}\right)^{-1}\{\Delta(S-R)_{CO_2} + \Delta(S-R)_{O_3} + \Delta(S-R)_{H_2O} + \Delta(S-R)_{albedo} +$

1305 $\Delta(S-R)_{cloud} + \Delta(S-R)_{non-LTE} + \Delta dyn\}$ (A12)

1306
1307
1308 As described in the main text of this paper, we can solve Eq. (A12) for each of
1309 the terms on its right-hand side, based on the linear decomposition principle.
1310 This yields the partial temperature changes due to each specific process. The
1311 factors $\Delta(S-R)_{CO_2}$, $\Delta(S-R)_{O_3}$, $\Delta(S-R)_{H_2O}$, $\Delta(S-R)_{albedo}$ and

1312 $\Delta(S-R)_{cloud}$ in eqs (1-5) are calculated by inserting the output variables
1313 from WACCM in the radiation code of CFRAM. Here, one takes the output
1314 variables from the control run, apart from the variable that is related to the
1315 direct forcing or the feedback. The table below shows which variables have
1316 been taken from the perturbation runs for each feedback.
1317

Direct forcing/feedback	Changed variables in the radiation code
CO_2	CO_2

Ozone	O_3
Water vapour	Specific humidity
	Surface pressure
	Surface temperature
	Dew point temperature
Albedo	Downwelling solar flux at surface
	Net solar flux at surface
Cloud	Cloud fraction
	Cloud ice
	Cloud liquid amount

Table A1: The variables from the perturbation runs inserted in the radiation code of CFRAM to calculate the temperature change in response to the changes in CO_2, O_3, water vapour, cloud and albedo.

Acknowledgements

Competing interests

The authors have no competing interests to declare.

References

Akmaev, R.A., Fomichev, V.I. and Zhu, X.: Impact of middle-atmospheric composition changes on greenhouse cooling in the upper atmosphere, *Journal of Atmospheric and Solar-Terrestrial Physics*, 68, 1879-1889, doi:10.1016/j.jastp.2006.03.008, 2006.

Beig, G., et al.: Review of mesospheric temperature trends, *Reviews of Geophysics,* 41(4), doi:10.1029/2002RG000121, 2003.

Bony, S., and co-authors: How well do we understand and evaluate climate change feedback processes?, *Journal of Climate*, 19(15), 3445–3482, doi:10.1175/JCLI3819.1, 2006.

Boucher, O., Randall, D., and co-authors: Clouds and Aerosols, in: *Climate Change: The Physical Science Basis. Contribution of Working Group I to IPCC AR5*, edited by: Stocker T.F. and coauthors., Cambridge University Press, Cambridge, United Kingdom and New York, NY, USA, 2013.

33

Brasseur, G. P., and Solomon, S.: Aeronomy of the middle atmosphere, Chemistry and physics of the stratosphere, Springer, New York, 2005.

Brewer, A. W.: Evidence for a world circulation provided by the measurements of helium and water vapour distribution in the stratosphere. *Quarterly Journal of the Royal Meteorological Society*, *75*(326), 351-363, doi:10.1002/qj.49707532603, 1949.

Brühl, C., & Crutzen, P. J.: Scenarios of possible changes in atmospheric temperatures and ozone concentrations due to man's activities, estimated with a one-dimensional coupled photochemical climate model, *Climate Dynamics*, *2*(3), 173-203, doi: /10.1007/BF01053474, 1988.

Butchart, N., and co-authors: Chemistry–climate model simulations of twenty-first century stratospheric climate and circulation changes, *Journal of Climate*, 23(20), 5349–5374, doi:10.1175/2010JCLI3404.1, 2010.

Caldwell, P.M., Zelinka, M.D., Taylor, K.E., Marvel, K.: Quantifying the sources of intermodal spread in equilibrium climate sensitivity, *Journal of Climate*, 29, 513-524, doi:10.1175/JCLI-D-15-0352.1, 2016.

Cai, M., and Lu, J.: A new framework for isolating individual feedback processes in coupled general circulation climate models. Part II: Method demonstrations and comparisons, *Climate dynamics*, 32(6), 887-900, doi:10.1007/s00382-008-0424-4, 2009.

Cariolle, D.: The ozone budget in the stratosphere: Results of a one-dimensional photochemical model, *Planetary and Space Science*, *31*(9), 1033-1052, doi:10.1016/0032-0633(83)90093-4, 1983.

Deckert, R. and Dameris, M.: Higher tropical SSTs strengthen the tropical upwelling via deep convection, *Geophysical Research Letters*, *35*(10), doi: 10.1029/2008GL033719, 2008.

Dobson, G. M. B.: Origin and distribution of the polyatomic molecules in the atmosphere. *Proceedings of the Royal Society of London. Series A. Mathematical and Physical Sciences*, *236*(1205), 187-193, doi:10.1098/rspa.1956.0127, 1956.

Fomichev, V.I., Jonsson, A.I., De Grandpre, J., Beagley, S.R., McLandress, C., Semeniuk, K., Shepherd, T.G.: Response of the middle atmosphere to CO_2 doubling: Results from the Canadian Middle Atmosphere Model, *Journal of Climate*, 20(7), 1121-1141, doi:10.1175/JCLI4030.1, 2007.

Fu, Q., and Liou, K. N.: On the correlated k-distribution method for radiative transfer in nonhomogeneous atmospheres. *Journal of the Atmospheric Sciences*, *49*(22), 2139-2156, doi:10.1175/1520-0469(1992)049<2139:OTCDMF>2.0.CO;2, 1992.

34

Fu, Q., and Liou, K. N.: Parameterization of the radiative properties of cirrus clouds. *Journal of the Atmospheric Sciences*, *50*(13), 2008-2025, doi: 10.1175/1520-0469(1993)050<2008:POTRPO>2.0.CO;2 1993.

Hu, X., Y. Li, S. Yang, Y. Deng and Cai. M.: Process-based decomposition of the decadal climate difference between 2002-13 and 1984-95, J. Climate, 30, 4373–4393, doi: 10.1175/JCLI-D-15-0742.1, 2017.

Hurrell, J.W., et al.: The Community Earth System Model: A framework for collaborative research. *Bulletin of the American Meteorological Society*, *94*(9), 1339-1360, doi: 10.1175/BAMS-D-12-00121.1, 2013.

Jaiser, R., K. Dethloff and Handorf, D.: Stratospheric response to Arctic sea ice retreat and associated planetary wave propagation changes, *Tellus A: Dynamic Meteorology and Oceanography*, 65(1), 19375, doi: 10.3402/tellusa.v65i0.19375, 2013.

Jonsson, A.I., de Grandpré, J., Fomichev, V.I., McConnell, J.C., Beagley, S.C.: Doubled CO_2-induced cooling in the middle atmosphere: Photochemical analysis of the ozone radiative feedback, *Journal of Geophysical Research*, 109, D24103, doi:10.1029/2004JD005093, 2004

Kinnison, D.E., Brasseur, G.P., Walters, S., Garcia, R.R. Marsh, D.R, Sassi, F., Harvey, V.L., Randall, C.E., Emmons, L., Lamarque, J.F., Hess, P., Orlando, J.J., Tie, X.X., Randall, W., Pan, L.L., Gettelman, A., Granier, C., Diehl, T., Niemeijer, Y., Simmons, A.J.: Sensitivity of chemical tracers to meteorological parameters in the MOZART–3 chemical transport model, *Journal of Geophysical Research: Atmospheres*, 112, D20302, doi:10.1029/2006JD007879, 2007.

Langematz, U.: Stratospheric ozone: down and up through the anthropocene, *ChemTexts* 5, 8, doi/10.1007/s40828-019-0082-7, 2019.

Lindzen, R.S.: Turbulence stress owing to gravity wave and tidal breakdown, *Journal of Geophysical Research: Oceans*, 86.C10, 9707–9714, doi:10.1029/JC086iC10p09707, 1981.

Lu, J., and Cai, M.: A new framework for isolating individual feedback processes in coupled general circulation climate model. Part I: Formulation. *Climate dynamics*, 32 (6), 873–885, doi:10.1007/s00382-008-0425-3, 2009.

Manabe, S., & Wetherald, R. T.: The effects of doubling the CO_2 concentration on the climate of a general circulation model. *Journal of the Atmospheric Sciences*, *32*(1), 3-15, 1975.

Marsh, D.R., Mills, M.J. Kinnison, D.E., Lamarque, J.F., Calvo, N., Polvani, L.M.: Climate change from 1850 to 2005 simulated in CESM1(WACCM), *Journal of Climate*, 26, 7372–7391, doi:10.1175/JCLI-D-12-00558.1, 2013.

1445 Marsh, D.R., Lamarque, J.-F., Conley, A.J. and Polvani, L.M., Stratospheric
1446 ozone chemistry feedbacks are not critical for the determination of climate
1447 sensitivity in CESM1(WACCM), *Geophysical Research Letters*, 43, 3928–
1448 3934, doi:10.1002/2016GL068344, 2016.

1449 McFarlane, N.A., The effect of orographically excited wave drag on the
1450 general circulation of the lower stratosphere and troposphere, *Journal of*
1451 *Atmospheric Sciences,* 44(14), 1775–1800,
1452 doi:10.1175/15200469(1987)044<1775:TEOOEG>2.0.CO;2, 1987.

1453 Neale, R., Richter, J., Park, S., Lauritzen, P., Vavrus, S., Rasch, P. and
1454 Zhang, M: The mean climate of the Community Atmosphere Model (CAM4) in
1455 forced SST and fully coupled experiments, *Journal of Climate*, 26, 5150–
1456 5168, doi:10.1175/JCLI- D-12-00236.1, 2013.

1457 Nowack, P.J., Abraham, N.L., Maycock, A.C., Braesicke, P., Gregory, J.M.,
1458 Joshi, M.M., Osprey, A., Pyle, J.A.: A large ozone-circulation feedback and its
1459 implications for global warming assessments, *Nature Climate Change*, 5 (1),
1460 41-45, 2015, doi:10.1038/NCLIMATE2451, 2015.

1461 Oberländer, S., Langematz, U. and Meul, S.: Unraveling impact factors for
1462 future changes in the Brewer-Dobson circulation, *Journal of Geophysical*
1463 *Research: Atmospheres*, 118, 10296-10312, doi:10.1002/jgrd.50775, 2013.
1464
1465 Ramaswamy, V., Collins, W., Haywood, J., Lean, J., Mahowald, N., Myhre,
1466 G., Naik, V., Shine, K.P., Soden, B., Stenchikov, G., Storelvmo, T., 2019:
1467 Radiative forcing of climate: The historical evolution of the radiative forcing
1468 concept, the forcing agents and their quantification, and application,
1469 *Meteorological Monographs* 59, 14.1 14.99,
1470 doi:10.1175/AMSMONOGRAPHS-D-19-0001.1
1471
1472 Ramaswamy, V., et al.: Stratospheric temperature trends: Observations and
1473 model simulations, *Reviews of Geophysics* 39.1, 71-122, doi:
1474 10.1029/1999RG000065, 2001.
1475
1476 Richter, J.H., Sassi, F., Garcia, R.R.: Toward a physically based gravity wave
1477 source parameterization in a general circulation model, *Journal of the*
1478 *Atmospheric Sciences*, 67, 136–156, doi:10.1175/2009JAS3112.1, 2010.

1479 Rieger, V.S., Dietmüller, S., Ponater, M.: Can feedback analysis be used to
1480 uncover the physical origin of climate sensitivity and efficacy differences?,
1481 *Climate Dynamics* 49, 2831-2844, doi: 10.1007/s00382-016-3476-x 2017.

1482 Riese, M., Ploeger, F., Rap, A., Vogel, B., Konopka, P., Dameris, M., &
1483 Forster, P.: Impact of uncertainties in atmospheric mixing on simulated UTLS
1484 composition and related radiative effects, *Journal of Geophysical Research:*
1485 *Atmospheres*, *117*(D16), doi:10.1029/2012JD017751, 2012.
1486

1487   Royer, J.F., Planton, S., Déqué, M.: A sensitivity experiment for the removal
1488   of Arctic sea ice with the French spectral general circulation model, *Climate*
1489   *Dynamics*, 5(1), 1-17, doi:10.1007/BF00195850, 1990.
1490
1491   Schmidt, H., Brasseur, G.P, Charron, M., Manzini, E., Giorgetta, M.A., Diehl,
1492   T., Fomichev, V., Kinnison, D., Marsh, D., Walters, S., The HAMMONIA
1493   Chemistry Climate Model: Sensitivity of the mesopause region to the 11-year
1494   solar cycle and CO_2 doubling, *Journal of Climate,* 19(16), 3903-3931,
1495   doi:10.1175/JCLI3829.1, 2006.
1496
1497   Shaw, T.A., and Shepherd T.G.: Atmospheric science: Raising the
1498   roof, *Nature geoscience,* 1(1), 12, doi:10.1038/ngeo.2007.53, 2008.

1499   Shepherd, T.G.: Dynamics, stratospheric ozone and climate change,
1500   *Atmosphere-Ocean*, 46,1, 117-138, doi:10.3137/ao.460106, 2008.

1501   Shepherd, T.G., and McLandress, C.: A robust mechanism for strengthening
1502   of the Brewer–Dobson circulation in response to climate change: critical layer
1503   control of subtropical wave breaking, *Journal of the Atmospheric Sciences*,
1504   68, 4, 784-797, doi:10.1175/2010JAS3608, 2011.

1505   Shine, K. P., et al.: A comparison of model-simulated trends in stratospheric
1506   temperatures, *Quarterly Journal of the Royal Meteorological Society: A journal*
1507   *of the atmospheric sciences, applied meteorology and physical*
1508   *oceanography* 129(590),1565-1588, doi:10.1256/qj.02.186, 2003.
1509
1510   Sigmond, M., Siegmund, P.C., Manzini, E. and Kelder, H.: A simulation of the
1511   separate climate effects of middle-atmospheric and tropospheric CO_2
1512   doubling, *Journal of Climate*, 17(12), 2352-2367, doi:10.1175/1520-
1513   0442(2004)017<2352:ASOTSC>2.0.CO;2, 2004.

1514   Soden, B., Held, I.M.,: An assessment of climate feedbacks in coupled ocean-
1515   atmosphere models, *Journal of Climate*, 19, 3354-3360,
1516   doi:10.1175/JCLI3799.1, 2006.

1517   Solomon, S., Rosenlof, K. H., Portmann, R. W., Daniel, J. S., Davis, S. M.,
1518   Sanford, T. J., & Plattner, G. K.: Contributions of stratospheric water vapor to
1519   decadal changes in the rate of global warming, *Science*, *327*(5970), 1219-
1520   1223, doi: 10.1126/science.1182488, 2010.
1521
1522   Song, X., and Zhang, G.J.: Role of climate feedback in El Niño-like SST
1523   response to global warming, *Journal of Climate*, 27, 7301–7318,
1524   doi:10.1175/JCLI-D-14-00072.1, 2014
1525
1526   Taylor, P.C., Cai, M., Hu, A., Meehl, J., Washington, W. and Zhang, G.J.: A
1527   decomposition of feedback contributions to polar warming amplification,
1528   *Journal of Climate*, 26, 7023–7043, doi:10.1175/JCLI-D-12-00696.1, 2013.
1529

1530 WMO (World Meteorological Organization), *Scientific Assessment of Ozone*
1531 *Depletion: 2018*, Global Ozone Research and Monitoring Project – Report No.
1532 58, 588 pp., Geneva, Switzerland, 2018.
1533
1534 Zhang, P., Wu, Y., Simpson, I.R., Smith, K.L., Zhang, X., De, B., and
1535 Callaghan, P.: A stratospheric pathway linking a colder Siberia to Barents-
1536 Kara Sea sea ice loss, *Science Advances*, 4(7), eaat6025, doi:
1537 10.1126/sciadv.aat6025, 2018.
1538
1539 Zheng, J., Zhang, Q., Li, Q., Zhang, Q. and Cai, M., Contribution of sea ice
1540 albedo and insulation effects to Arctic amplification in the EC-Earth Pliocene
1541 simulation*, Climate of the Past*, 15, 291-305, doi:10.5194/cp-15-291-2019,
1542 2019.
1543
1544 Zhu, X., Yee, J.-H., Cai, M., Swartz, W.H., Coy, L., Aquila, V., Garcia, R.,
1545 Talaat, E.R.: Diagnosis of middle-atmosphere climate sensitivity by the
1546 climate feedback-response analysis method, *Journal of Atmospheric*
1547 *Sciences*, 73(1), 3-23, doi:10.1175/JAS-D-15-0013.1, 2016.